Contract No:

This document was prepared in conjunction with work accomplished under Contract No. 89303321CEM000080 with the U.S. Department of Energy (DOE) Office of Environmental Management (EM).

Disclaimer:

This work was prepared under an agreement with and funded by the U.S. Government. Neither the U.S. Government or its employees, nor any of its contractors, subcontractors or their employees, makes any express or implied:

1) warranty or assumes any legal liability for the accuracy, completeness, or for the use or results of such use of any information, product, or process disclosed; or
2) representation that such use or results of such use would not infringe privately owned rights; or
3) endorsement or recommendation of any specifically identified commercial product, process, or service.

Any views and opinions of authors expressed in this work do not necessarily state or reflect those of the United States Government, or its contractors, or subcontractors.

SRNL-STI-2022-00595

Defect-related carrier transport in CdTe-based compounds: comparison with hybrid perovskites

Jan Franc[1], Václav Dědič[1], Roman Grill[1], Martin Rejhon[1,2], Eduard Belas[1], Jindřich Pipek[1], Petr Praus, Utpal N. Roy[3], Ralph James[3] and Paul Sellin[4]

1) Faculty of Mathematics and Physics, Charles University, Ke Karlovu 5, CZ-121 16, Prague 2, Czech Republic

2) Tandon School of Engineering, New York University, Brooklyn, NY 11201, USA

3) Savannah River Natl Lab, Aiken, SC 29808 USA

4) Univ Surrey, Dept Phys, Guildford GU2 7XH, Surrey, England

RTSD Workshop, Milano, November 10, 2022

Thanks:

Group in Prague:

V. Dědič, M. Rejhon , R. Grill, E. Belas, P. Moravec, P. Höschl, P. Praus, J. Pipek,
M. Betušiak, R. Fesh, J. Kubát, H. Elhadidy

Main collaborating groups:

- Brookhaven National Laboratory, R.B. James, U. N. Roy, K.H.Kim, A. Bolotnikov, Ge Yang, R.Gul, G. Camarda
- Savannah River National Laboratory – R.B. James, U. N. Roy
- Freiburger Materialforschungszentrum (FMF) – M. Fiederle, A. Fauler, V. Babentsov
- University of Surrey – P. Sellin
- IMEM, Parma – A. Zappettini
- University of Bologna – B. Fraboni, A. Cavallini
- Korea University – K.H.Kim
- Redlen technologies – G. Prekas, K. Iniewski

History of CdTe crystal growth and defect studies at the Institute of Physics, Charles University

1962 – 1st paper (Growing of CdTe single crystals by static sublimation.., P.Höschl, C.Konak, Czech.J.Phys.)

1977 –paper P. Höschl et al., Rev.Phys.Appl.

1985 –2002 HgCdTe bulk crystals for infrared detectors
CdZnTe crystals as substrates for HgCdTe MBE epitaxial layers

CdTe
CdZnTe
CdZnTeSe

For X-ray and gamma-ray detectors

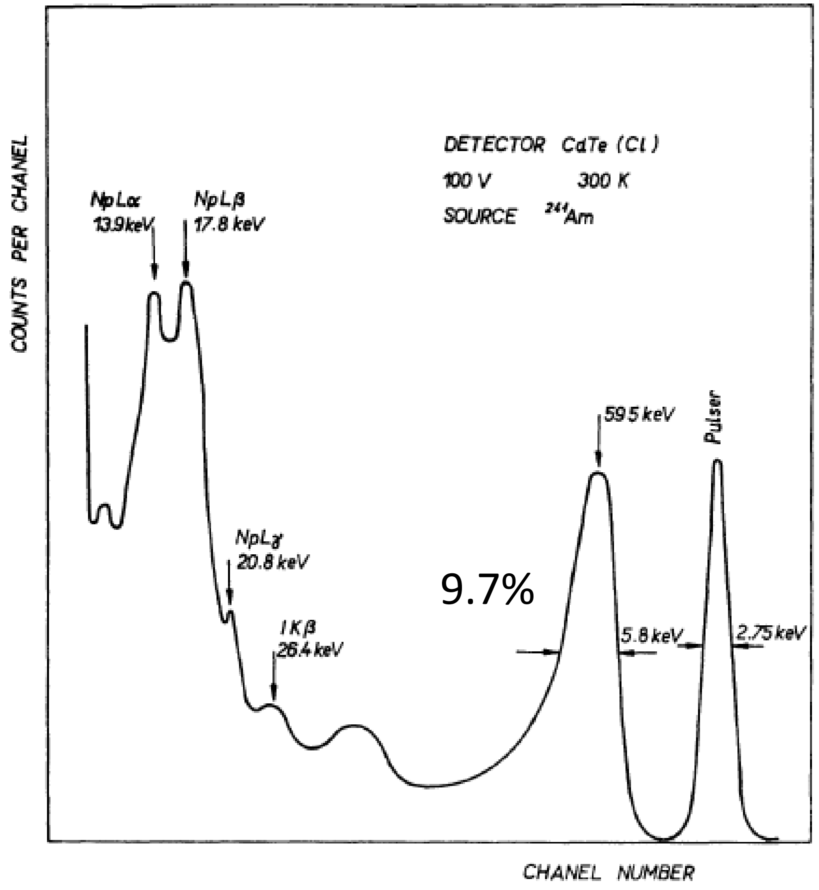

FIG. 5. — ^{241}Am gamma-ray spectrum at room temperature.

Defects and their impact on detector performance

Methods

photoluminescence

TEES, PICTS

photoconductivity

Pockels effect

Transient current technique
(L-TCT)

Photo-Hall effect spectroscopy

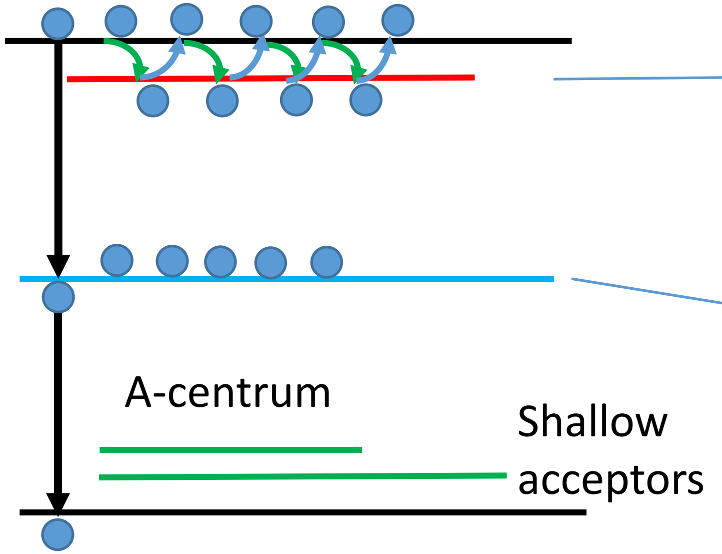

Shallow donors
(In, Cl)

+ **compensation**
semi-insulating
state

- **trapping/retrapping**
decrease of effective
mobility of electrons

Deep levels

+ **compensation**
semi-insulating
state

- **trapping/recombination**
loss of free charges
buildup of space charge

Achievement of the semi-insulating state

$N_D \sim 10^{15} cm^{-3}$

$N_{DEEP} \sim 10^{11} cm^{-3}$

$\sigma \sim 10^{-13} - 10^{-14} cm^2$

$N_A \sim 10^{15} cm^{-3}$

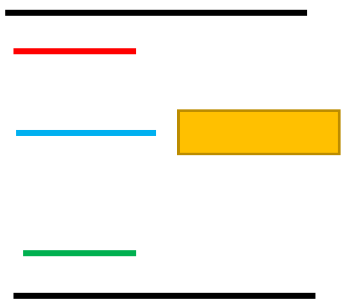

Fermi energy

$N_{DEEP} > |N_D - N_A| \, cm^{-3}$

In_{Cd}

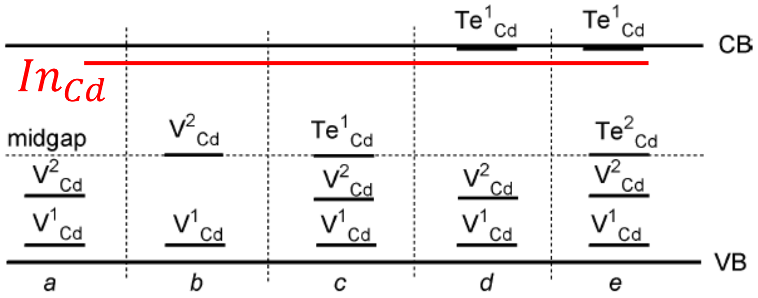

R. Grill, J. Franc, P. Höschl, I. Turkevych, E.Belas, P. Moravec, IEEE Trans.Nucl.Sci. 52, 1925, 2005.

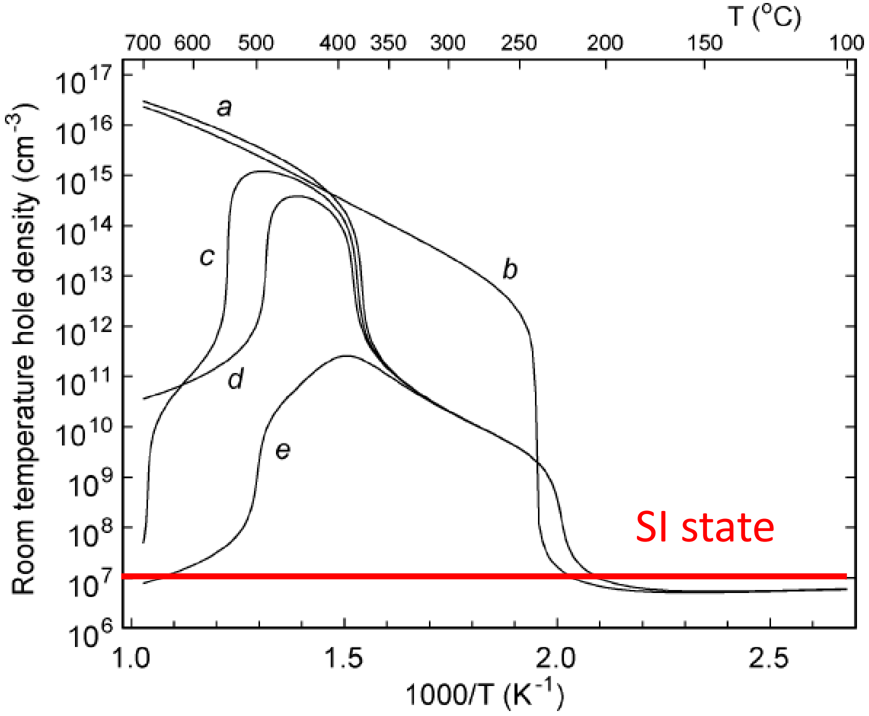

$V_{Cd}, Te_{Cd} \rightarrow Te_{ppt}$

Model

Slow cooling at Te-rich conditions

Reduction of point defects by precipitation

Semi-insulating state is achieved at ~200K

Midgap level

$$\tau_{t,e} = \frac{1}{\sigma_e v_{th} N_t f} \qquad f = \frac{1}{1 + e^{E_t - E_F}}$$

Weak N-type

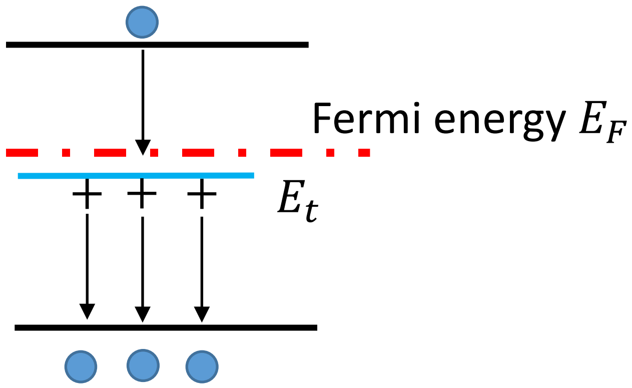

Weak electron trapping,
Good electron mobility

Strong hole trapping,
Buildup of positive
space charge

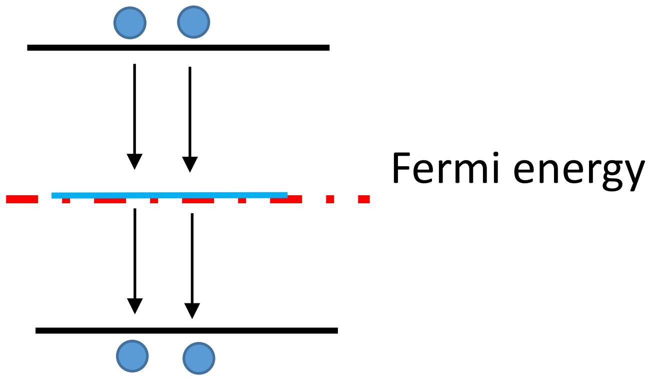

Recombination center

Due to a higher electron than hole mobility trapping of electrons is weaker than the trapping of holes

Weak P-type

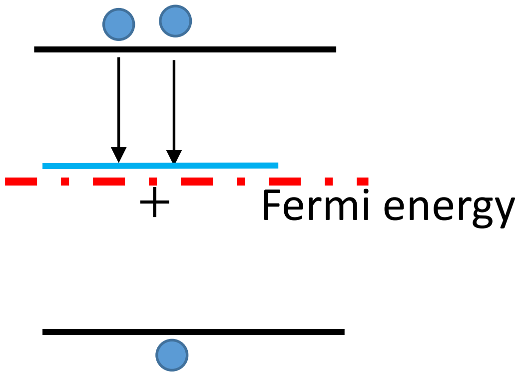

Moderate electron trapping
Weak hole trapping

Typical CdZnTeSe ingots (SRNL)

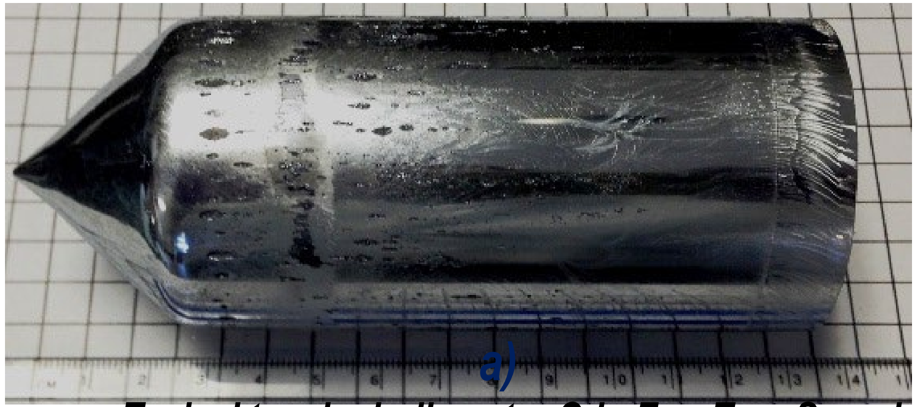

a)

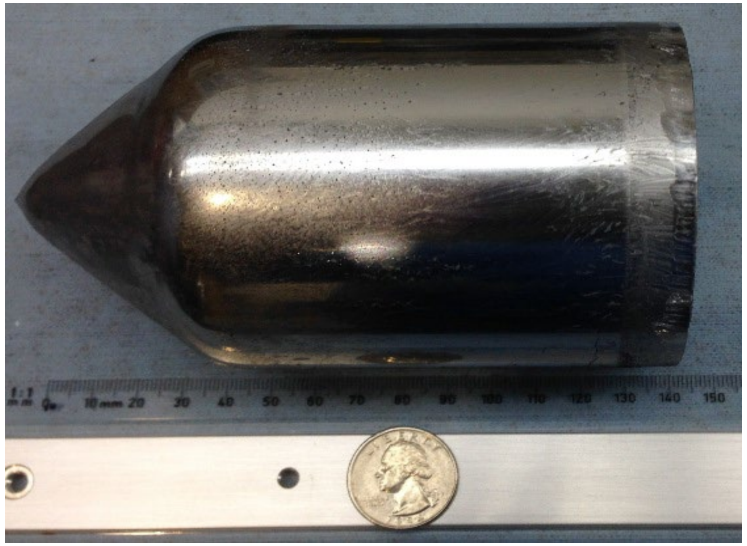

b)

Typical two-inch diameter $Cd_{0.9}Zn_{0.1}Te_{0.98}Se_{0.02}$ ingot grown by Traveling Heater Method (THM) a) two-inch and b) three-inch diameter.

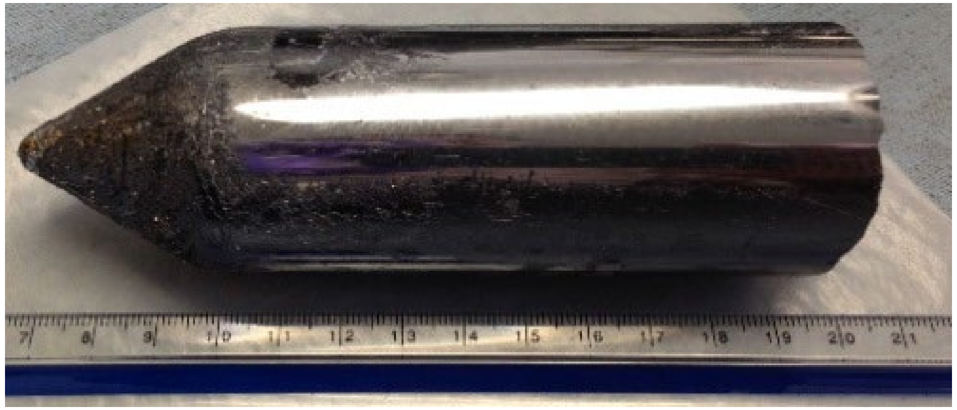

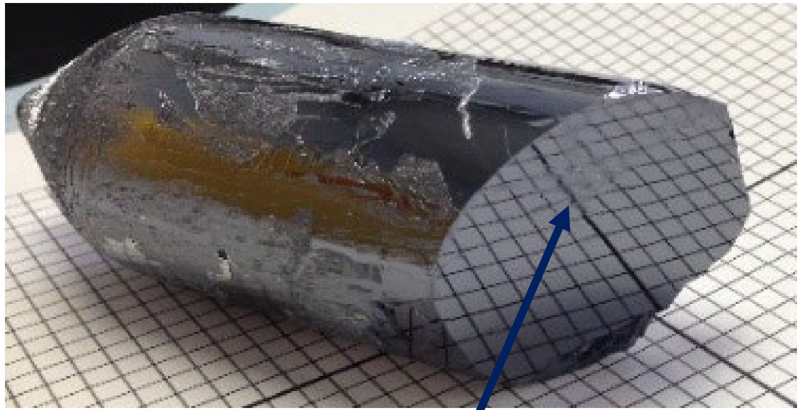

40-mm diameter ingot grown by Bridgman growth technique (undoped).

Cleaved surface

Electric field measurements – Pockels effect

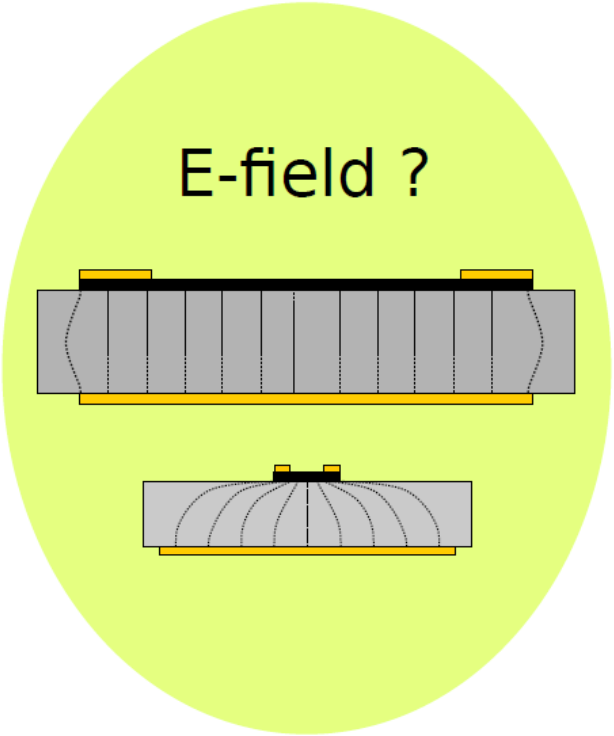

Gauss law: E-field $\Longleftrightarrow$ space charge

CdTe, CdZnTe, CdZnTeSe ... optically isotropic crystals of $\overline{4}3m$ symmetry (FCC) showing Pockels effect (E-field induced **birefringence**)

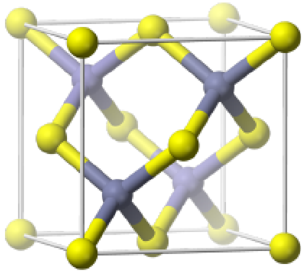

E-field	Crystal
0	isotropic
$\neq 0$	anisotropic

Taylor:

$$n(E) = n + a_1 E + \frac{1}{2} a_2 E^2 + \ldots$$

with electrooptic coefficients r and s:

$$n(E) \approx n - \frac{1}{2} r n^3 E - \frac{1}{2} s n^3 E^2$$

Pockels effect (linear)

Kerr effect (quadratic)

Pockels effect – arbitrary direction of E-field

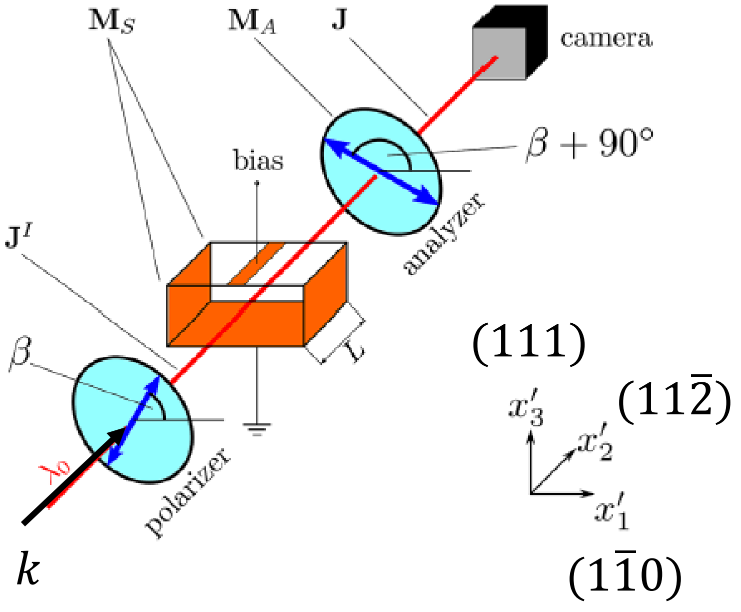

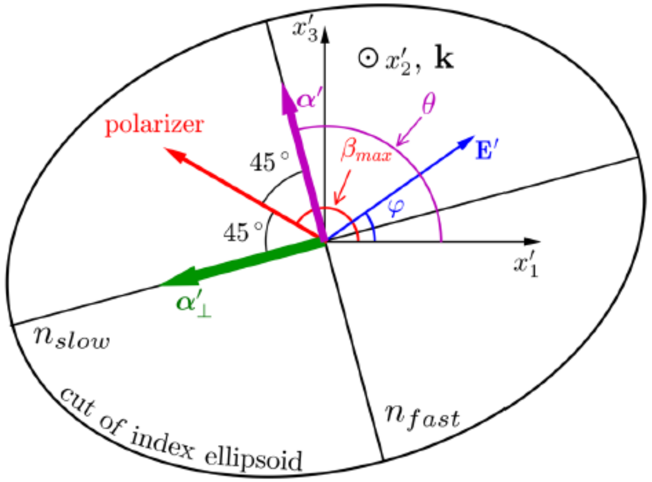

We measure transmission

$$T(E) = sin^2 \frac{\Gamma(E)}{2} sin^2[2(\beta-\theta)]$$

Phase shift

$$\Gamma(E) = \frac{2\pi}{\lambda_0}[n_{fast} - n_{slow}]L$$

if $\beta = \Theta + \frac{\pi}{4}$, then

$$T_{max}(E) = sin^2 \frac{\Gamma(E)}{2}$$

β - the angle of polarizer from x'_1

Θ –the angle of fast axis from x'_1

Θ depends on the direction of E-field

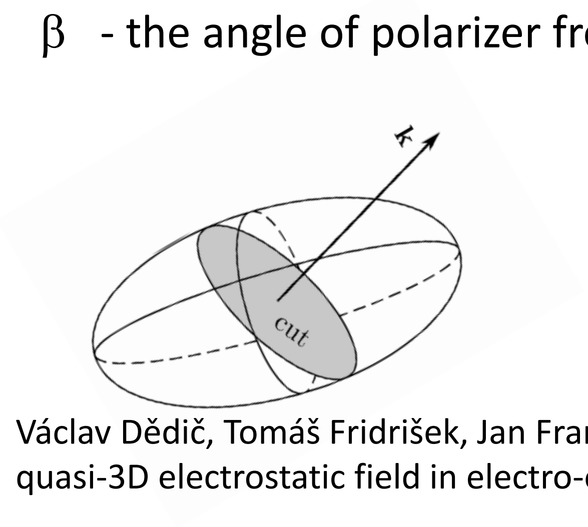

Václav Dědič, Tomáš Fridrišek, Jan Franc, Jan Kunc, Martin Rejhon, Utpal N. Roy, Ralph B. James, Mapping of inhomogenous quasi-3D electrostatic field in electro-optic materials, Scientific Reports (2021) 11:2154

Mapping of electric fields

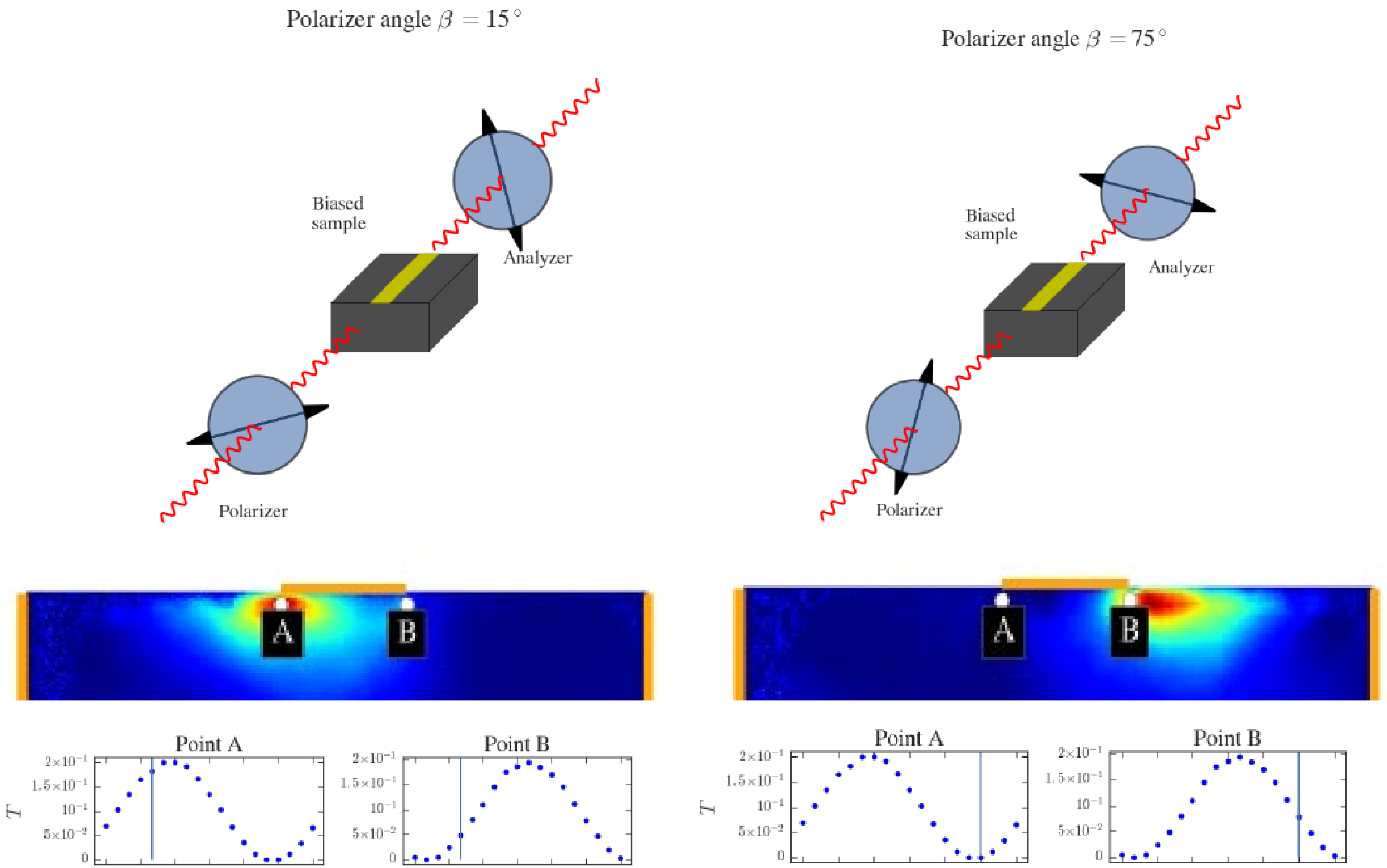

$$T(E) = sin^2\frac{\Gamma(E)}{2} sin^2[2(\beta-\theta)]$$

Evaluation of the E-field map:

1. Each pixel must be treated as a separate sample
2. Maximum of transmission T is found rotating the crossed polarizer-analyzer set
3. E-field calculated from

$$T_{max}(E) = sin^2\frac{\Gamma(E)}{2}$$

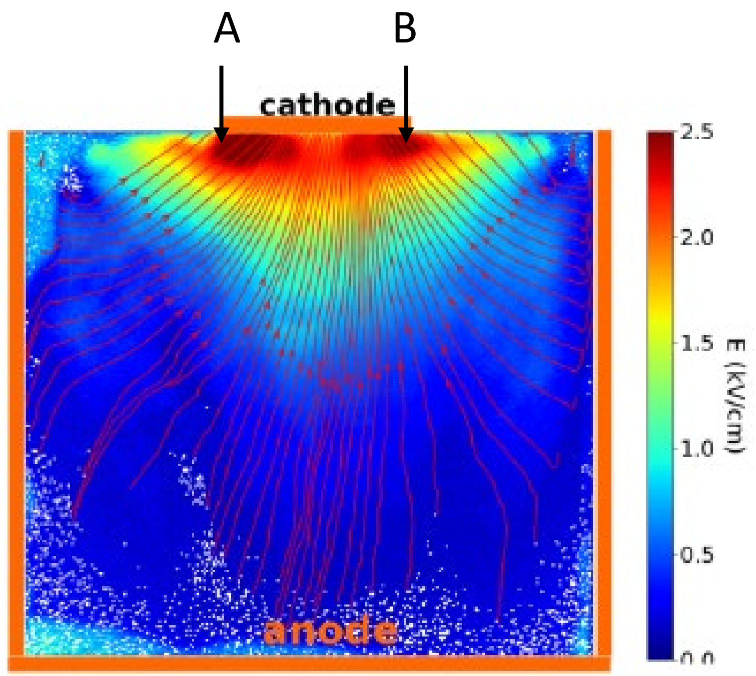

Pockels effect – E-field is parallel to (111)

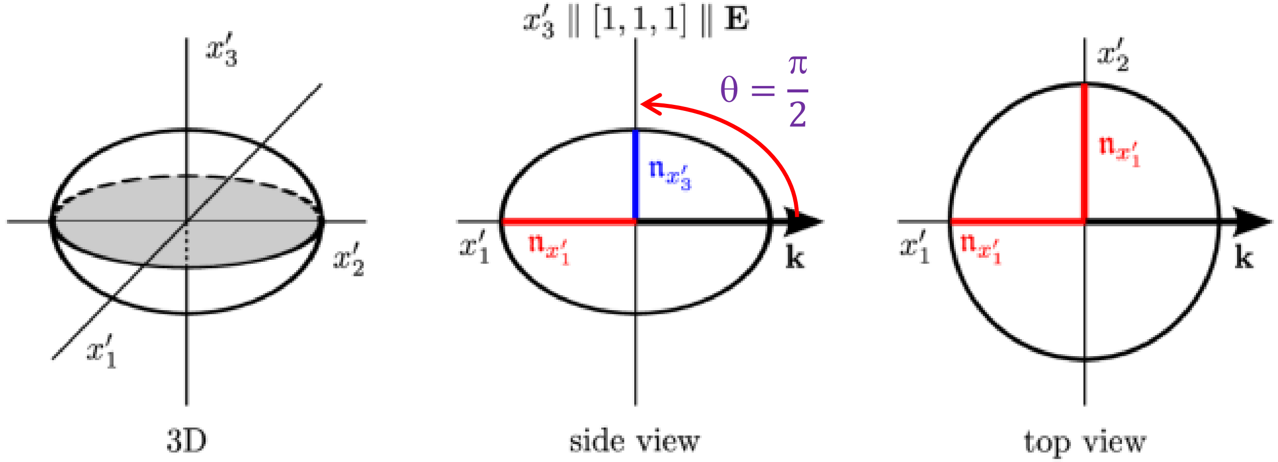

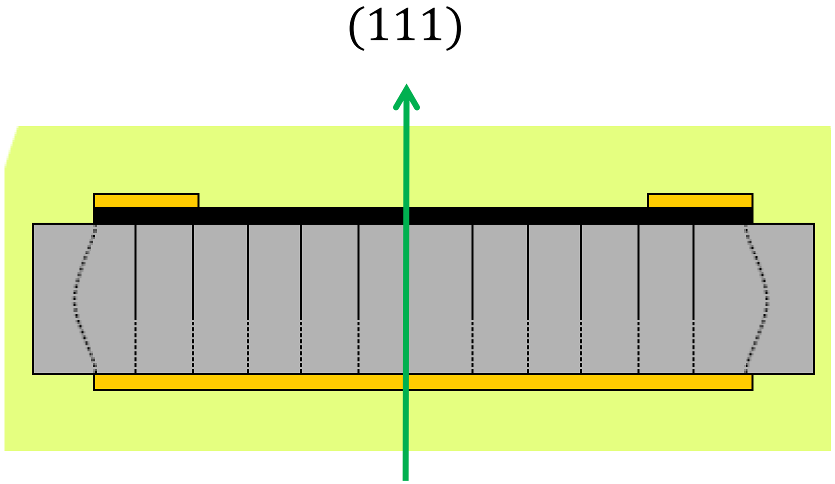

$\theta = \frac{\pi}{2}$, for $\beta = \frac{\pi}{4}$ → $2(\beta - \theta) = -\frac{\pi}{2}$ → $sin^2[2(\beta\text{-}\theta)]=1$ → $T(E) = T_{max}(E) = sin^2\frac{\Gamma(E)}{2}$

Simple situation, with polarizer angle $\beta = \frac{\pi}{4}$, analyzer angle $\beta = \frac{3\pi}{4}$, T_{max} is measured

Electric field evaluation

$$T = \sin^2\left(\frac{\sqrt{3}}{2}\frac{\pi r_{41} n_0^3 E L}{\lambda_0}\right) \Rightarrow E(x_1', x_3') = \frac{2}{\sqrt{3}}\frac{\lambda_0}{\pi r_{41} n_0^3 L} \arcsin\sqrt{T(x_1', x_3')} = \alpha_P \arcsin\sqrt{T(x_1', x_3')}$$

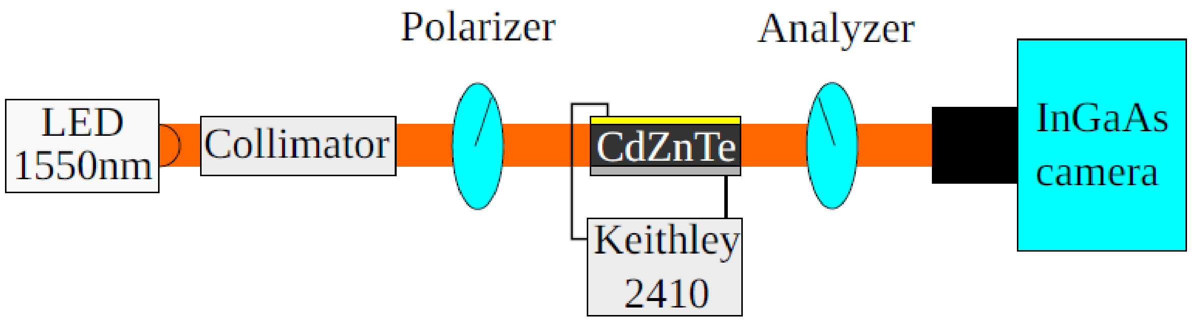

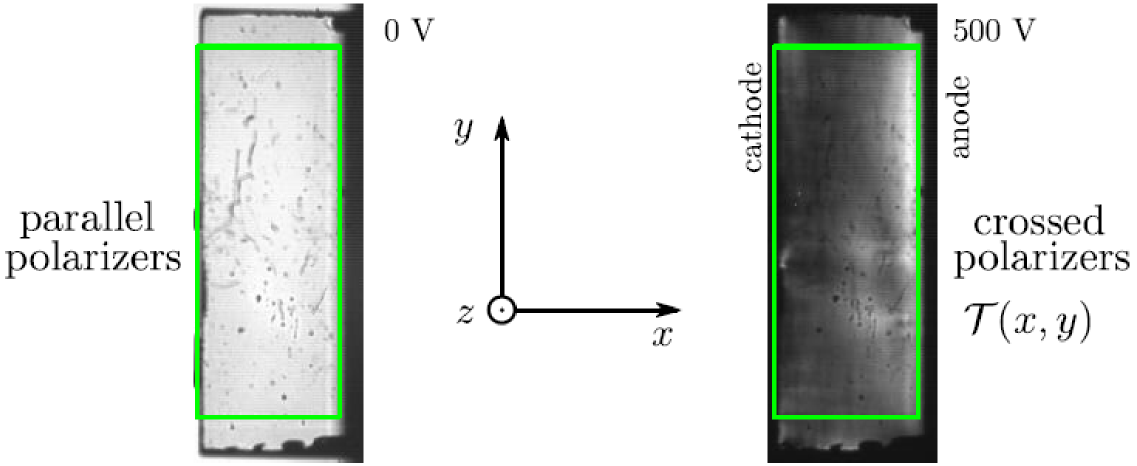

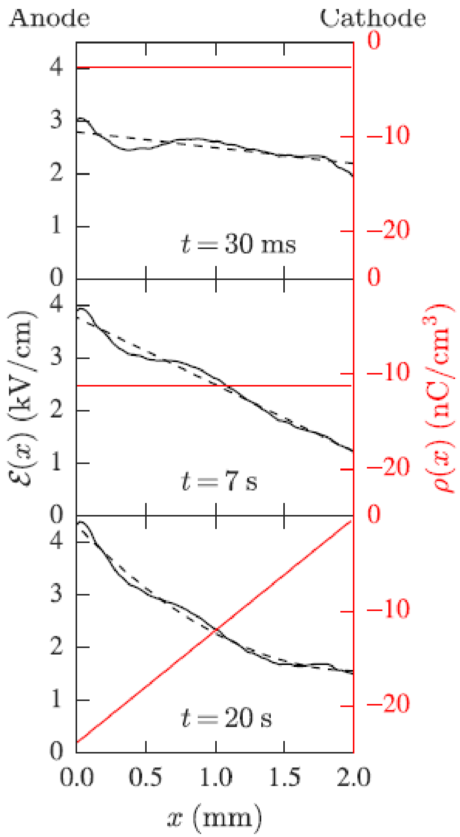

Space charge density

$$\rho(x) = \varepsilon \frac{\partial \mathcal{E}(x)}{\partial x}$$

Total space charge

$$Q = \int_V \rho(x) dV = S \int_a^c \rho(x) dx$$

$$\boxed{Q = \varepsilon S(\mathcal{E}_c - \mathcal{E}_a)}$$

Experimental methods based on Pockels effect I

E-field DLTS
(DLTS = deep level transient spectroscopy)

- Subject of study: thermal emission of carriers from traps
- Temporal and temperature dependence of the E-field (reflecting space charge) after switchin ON the bias or switching OFF the illumination (light assisted trap filling)
- Output: activation energy and capture cross-sections of traps (Arrhenius plot)$\Rightarrow$deep levels responsible for space charge accumulation
- Advantage: higher sensitivity than current techniques, direct space charge sign estimation

$$Q(t) = A \exp\left(-\frac{t}{\tau}\right) + Q^{\infty}.$$

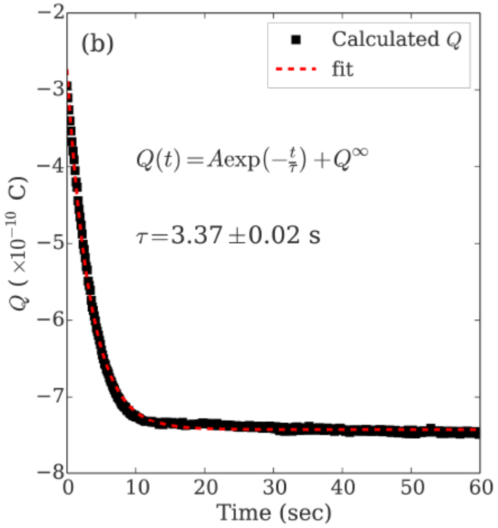

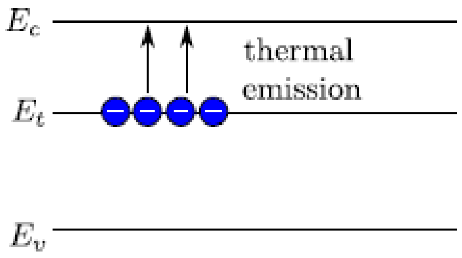

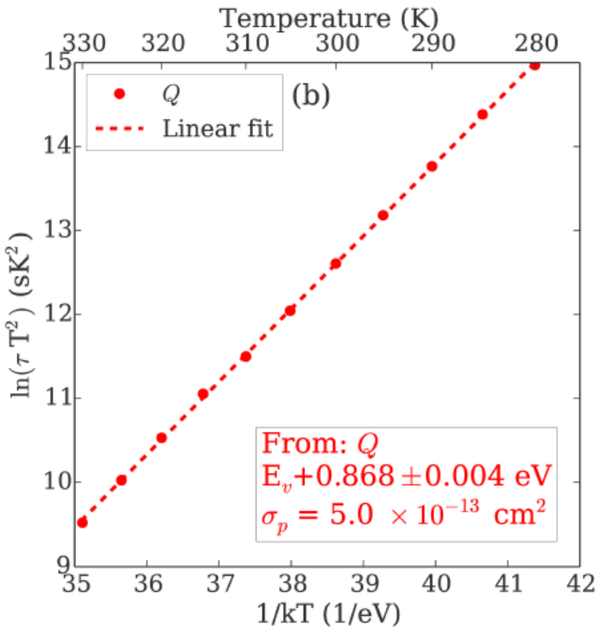

Arrhenius equation: $\ln(\tau T^2) = \frac{E}{kT} + \ln\left(\frac{C}{\sigma}\right)$ $\quad C = \frac{h^3}{16 m^*_{e(h)} \pi k_B^2}$

Determination of type of transitions

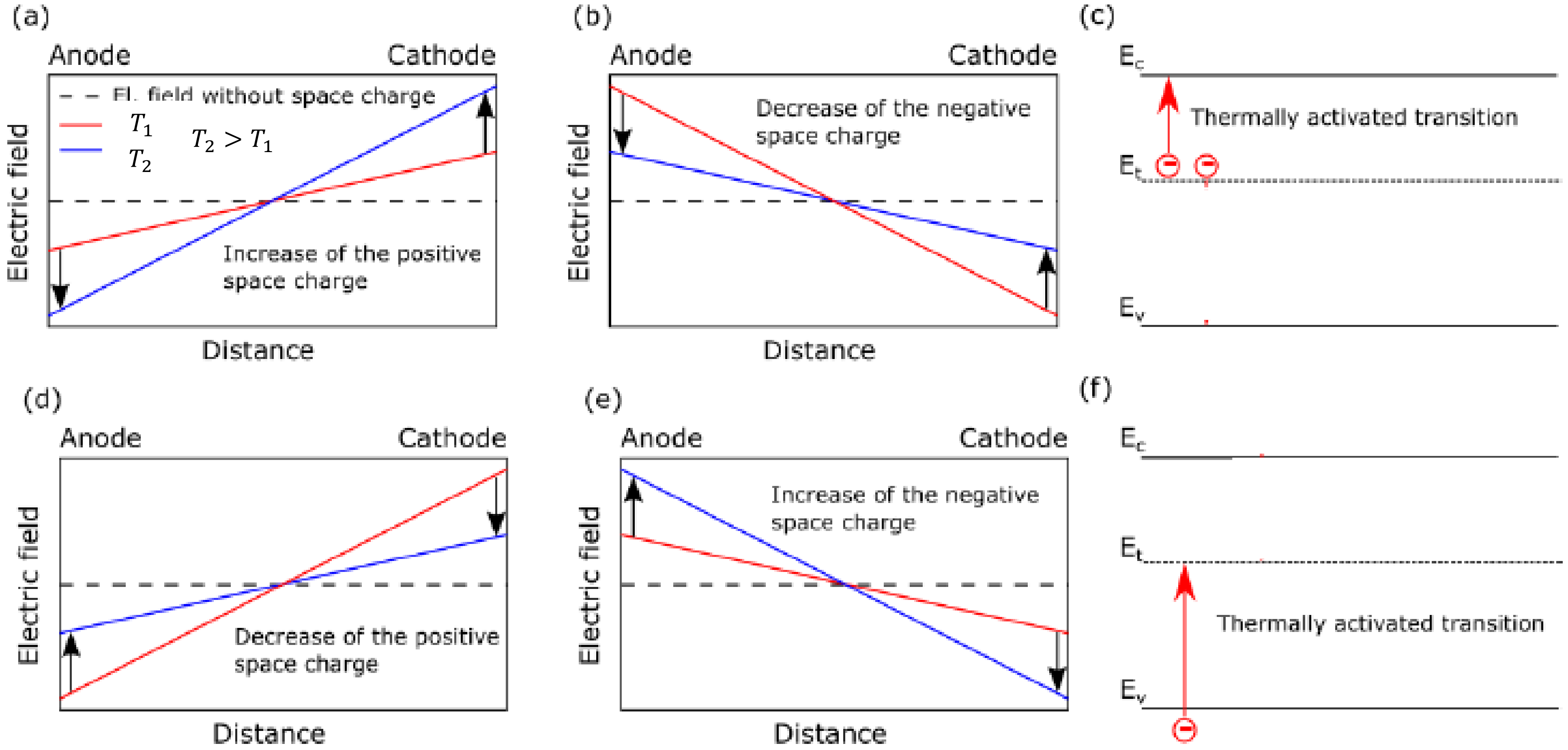

Photo generated space charge

Example (biased semiinsulating sample):

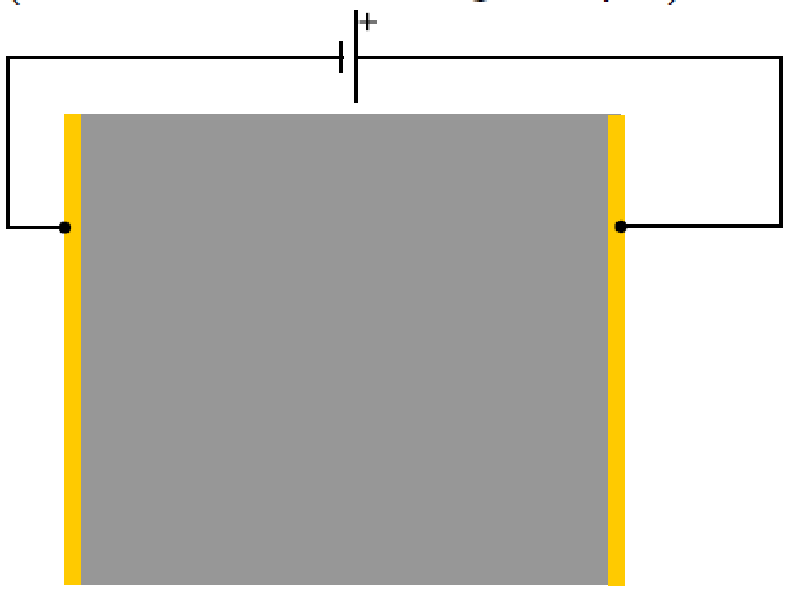

Main factors:

- defect structure (traps, optical transitions)
- penetration depth (photon energy)
- polarity (in case of low penetration)
- electrode material

Photo generated space charge

Example (biased semiinsulating sample):

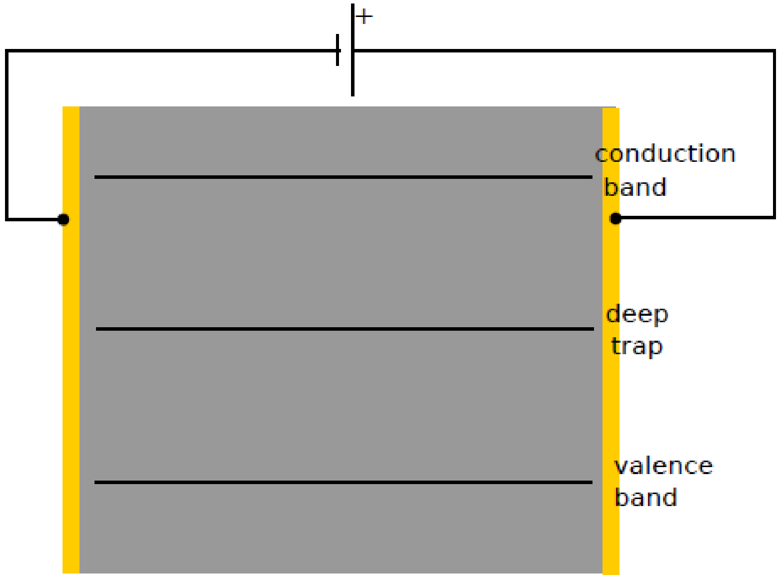

Main factors:

- defect structure (traps, optical transitions)
- penetration depth (photon energy)
- polarity (in case of low penetration)
- electrode material

Photo generated space charge

Example (biased semiinsulating sample):

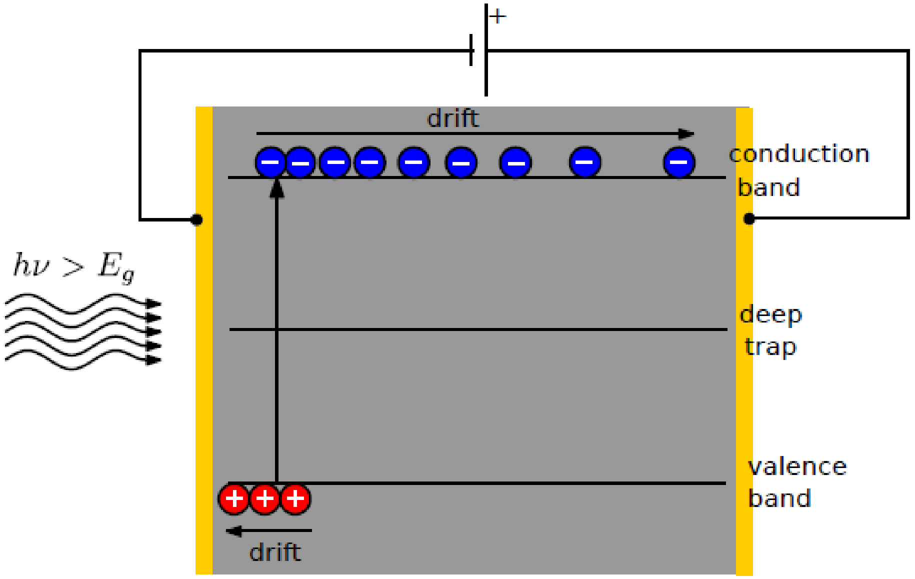

Main factors:

- defect structure (traps, optical transitions)
- penetration depth (photon energy)
- polarity (in case of low penetration)
- electrode material

Photo generated space charge

Example (biased semiinsulating sample):

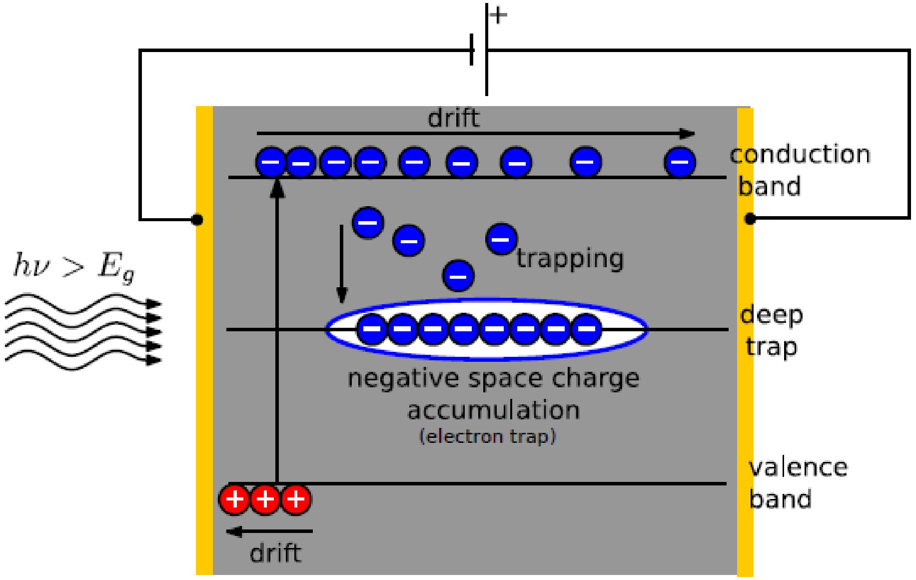

Main factors:

- defect structure (traps, optical transitions)
- penetration depth (photon energy)
- polarity (in case of low penetration)
- electrode material

Photo generated space charge

Example (biased semiinsulating sample):

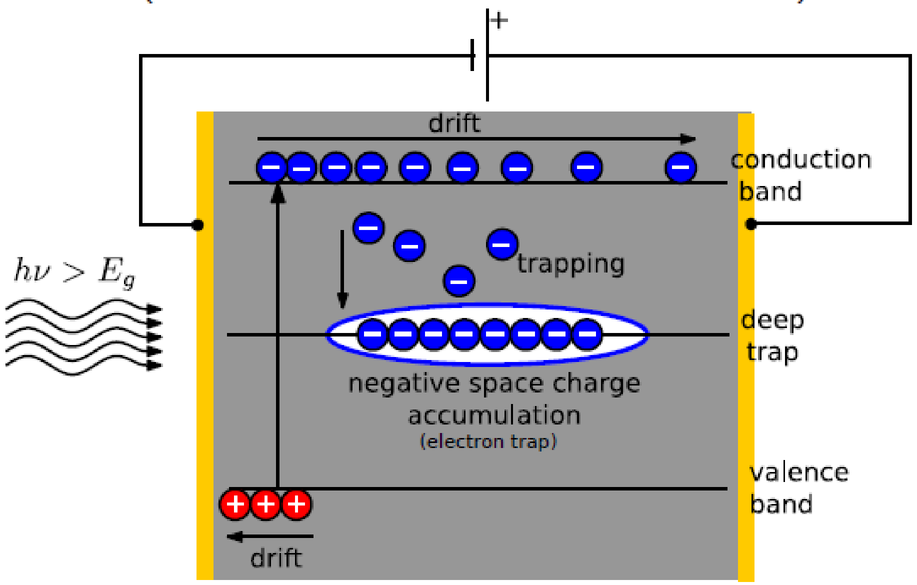

Main factors:

- defect structure (traps, optical transitions)
- penetration depth (photon energy)
- polarity (in case of low penetration)
- electrode material

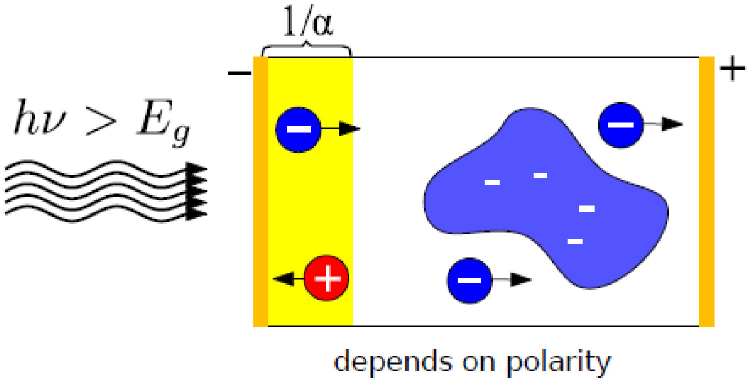

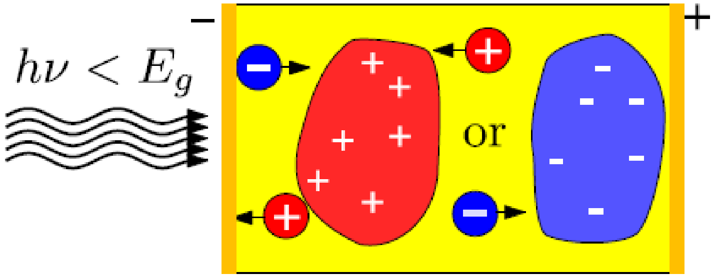

Experimental methods based on Pockels effect II

3-lights experiment
(infrared spectral scanning)

- Subject of study: optical transitions on deep levels
- Light sources:
  - Laser: band-to-band carrier generation (injection)⇒trap filling
  - Tunable monochromatic light: activation of optical transitions
  - Testing light: very low intensity, Pockels effect probe
- Output: E-field (charge) dependence on the photon energy reflecting the transitions enhanced by band-to-band generation (optical injection of carriers)⇒deep levels responsible for space charge accumulation
- Advantage: higher sensitivity than current techniques, direct space charge sign estimation

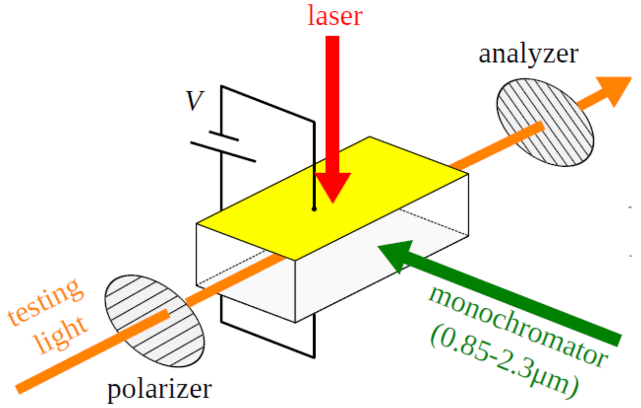

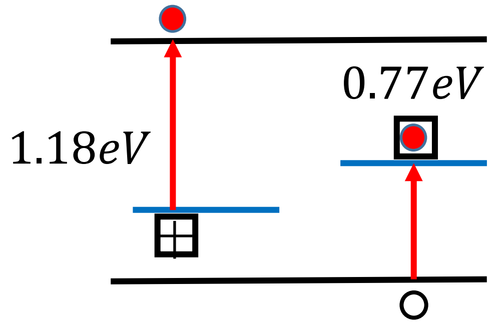

CZTS

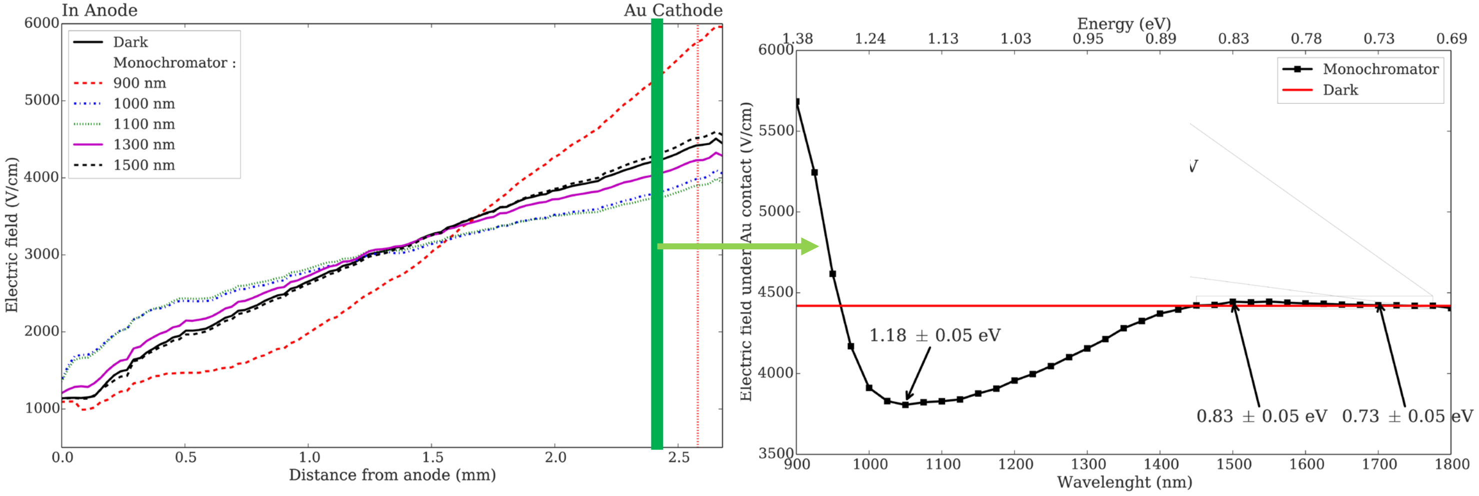

"De-polarization" of high-flux X-ray detector

- X-ray (tube at 80 kV) analogous e-h pair creation to band-to-band generation due to photoeffect
- significant positive space charge accumulation due to strong hole trapping ⇒ screening of the electric field (also "detector polarization")⇒ reduction of CCE
- optical transition reducing space charge⇒ detector recovery

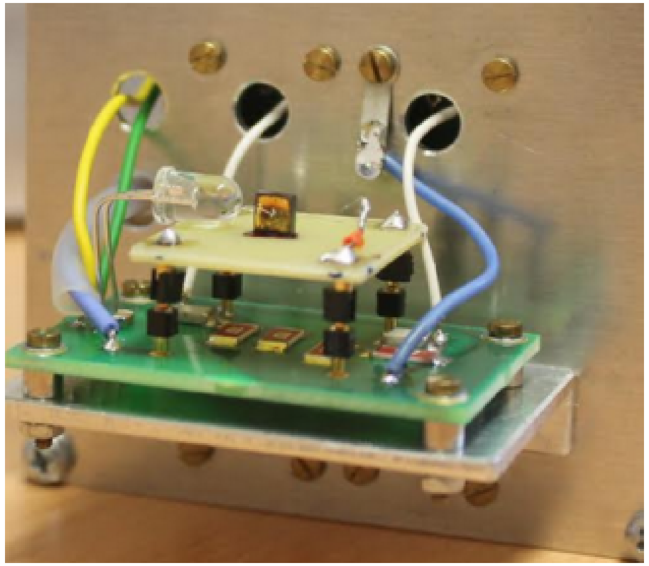

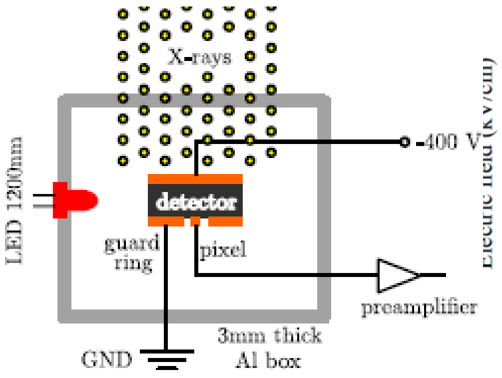

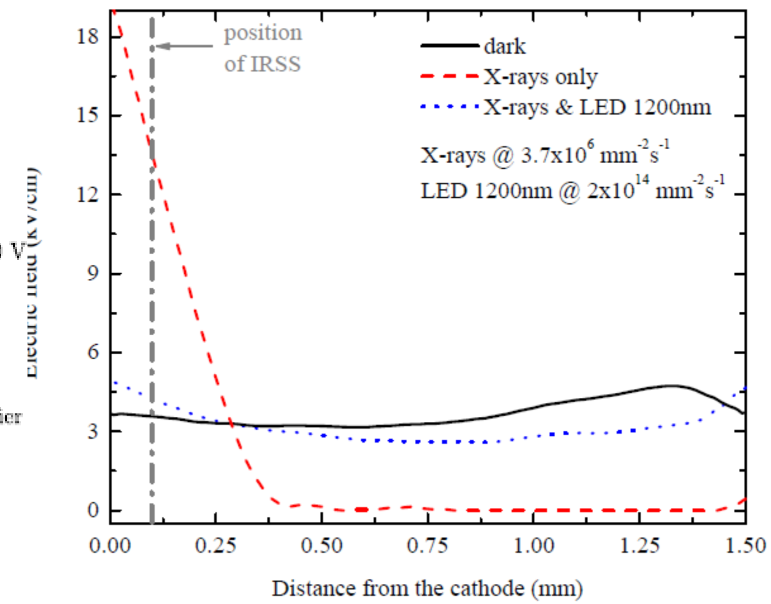

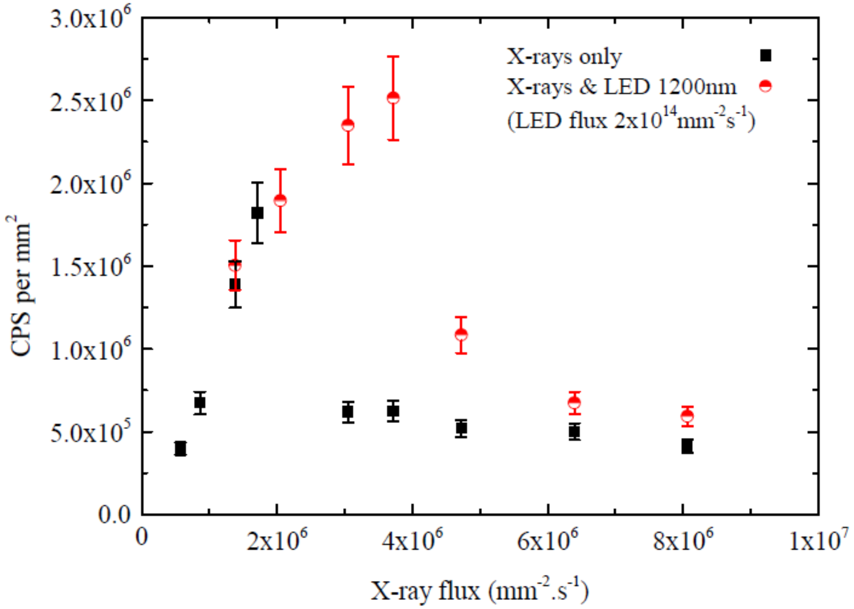

De-polarization at high fluxes

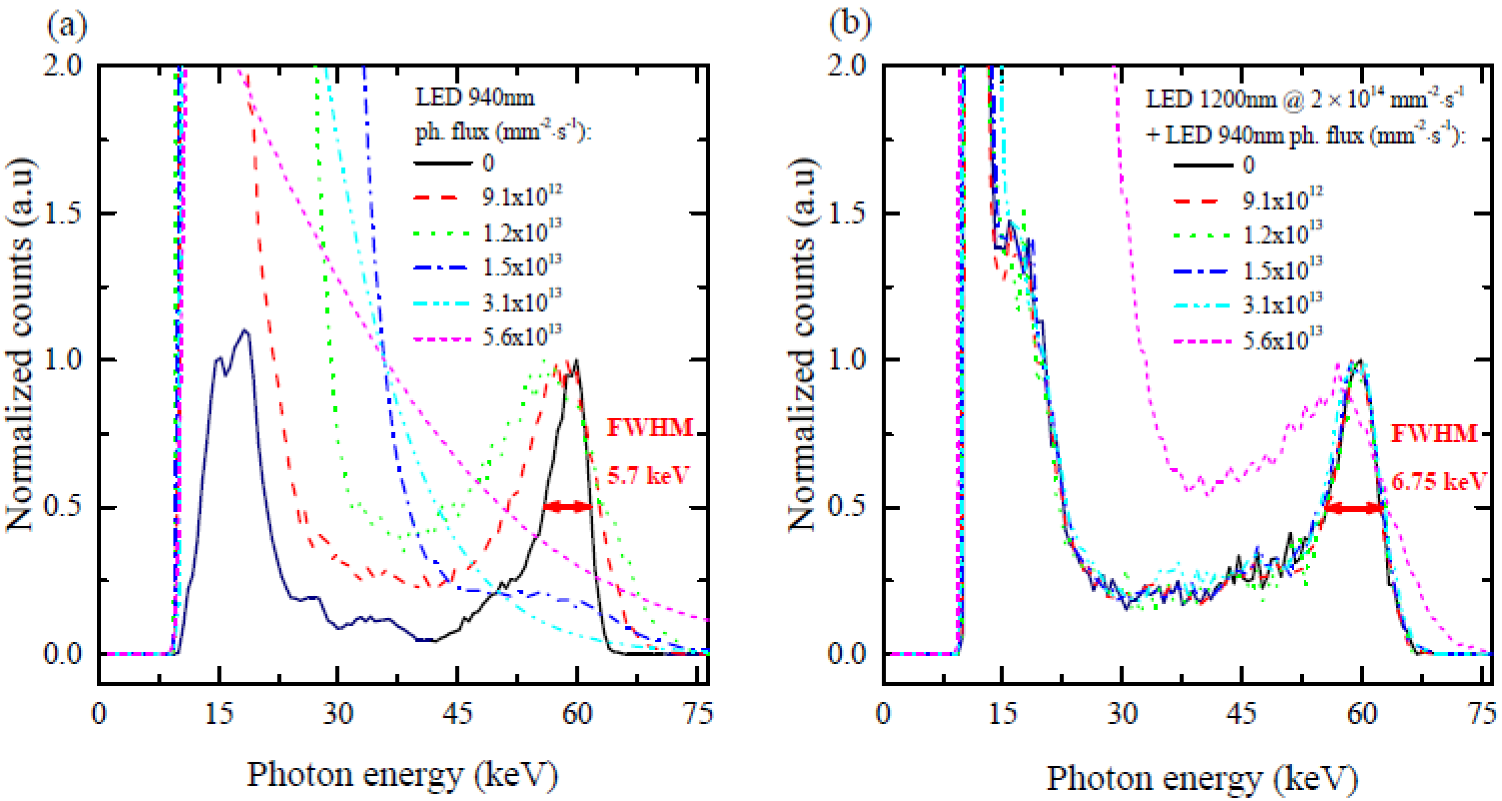

Pulse height spectra of γ-^{241} Am polarized by LED at 940nm (a) and with additional depolarization by led at 1200nm (b)

Summary of deep levels (Pockels effect)

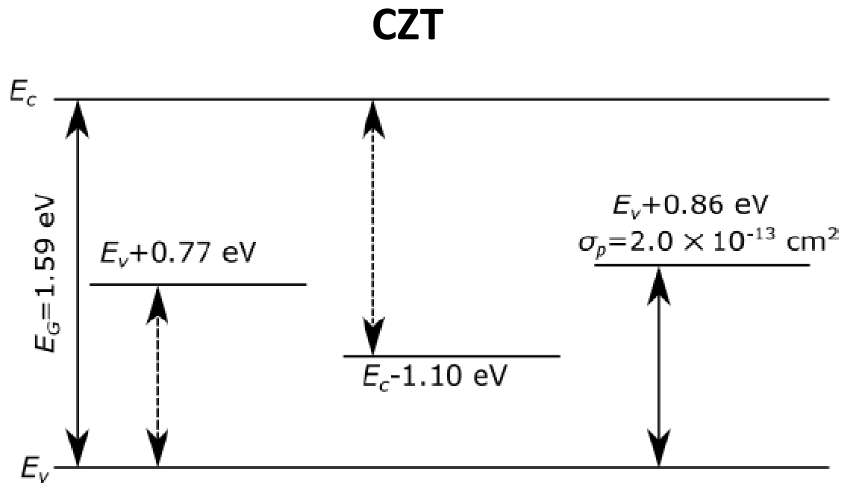

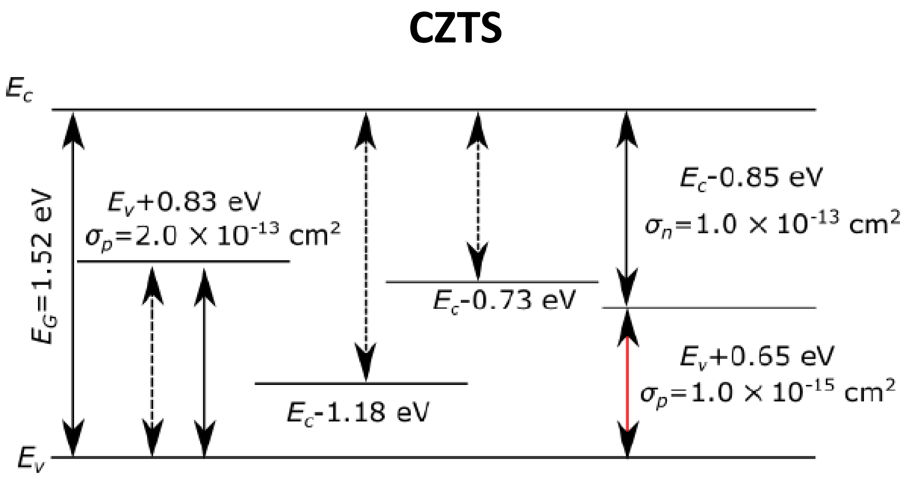

- ❑ Solid line – Time and temperature measurement
- ❑ Dashed line – Infrared spectral scanning
- ❑ Red line – Time and temperature current measurement

- ❑ E_c-1.10 (1.18) eV - causes optically induced polarization (Te inclusions/precipitates or Te vacancy)
- ❑ E_v+0.83 eV (CZTS) probably same origin as E_v+0.77 eV (CZT) (Cd vacancy)
  - ❑ The energy shift was theoretically predicted by Varley [1]
- ❑ E_c-0.85 eV (CZTS) – responsible for positive space charge
- ❑ E_v+0.86 eV (CZT) - responsible for negative space charge

Laser Induced Current Technique (L-TCT)

- Based on measuring the current response of the detector to a laser pulse
- Allows to characterize the charge transport (mobility, lifetime, electric field profile)
- Bias polarity selects which carrier type drift thought detector

L-TCT setup

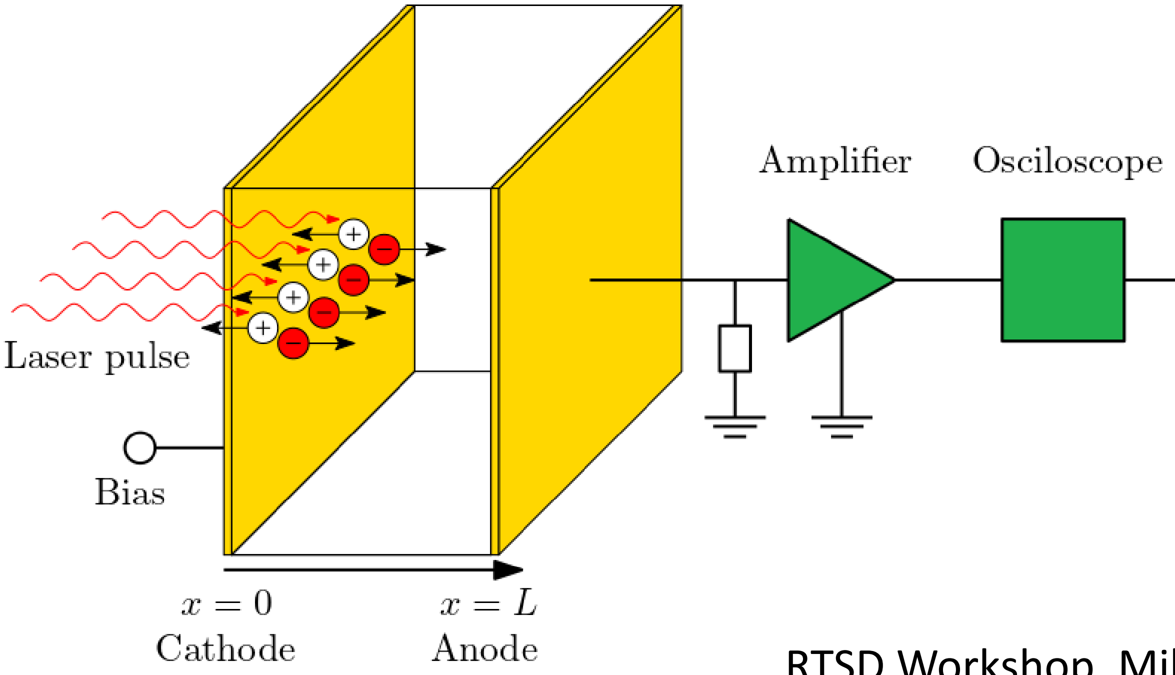

Current waveform

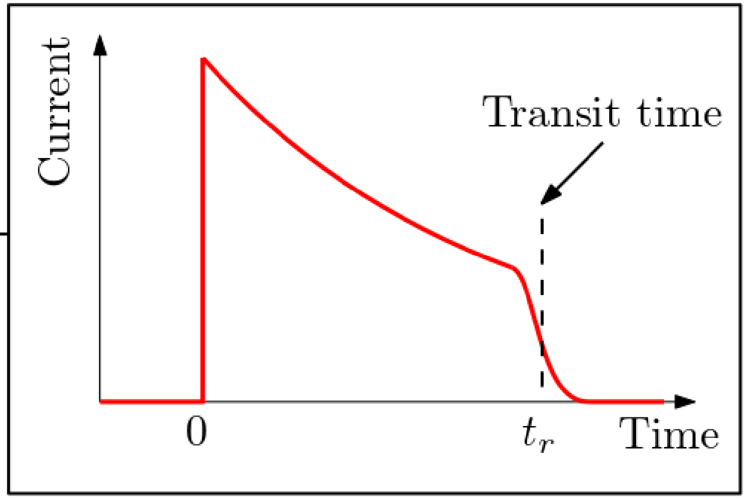

Monte Carlo Simulation

- 1D numerical simulation of charge transport in semiconductor detector
- Combined with numerical solution of drift-diffusion equation and Poisson’s equation
- allows study of charge transport and space charge dynamics

Band diagram

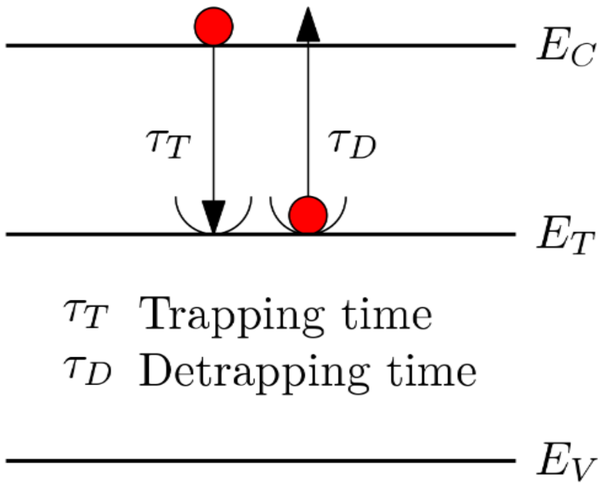

Detector

Current response

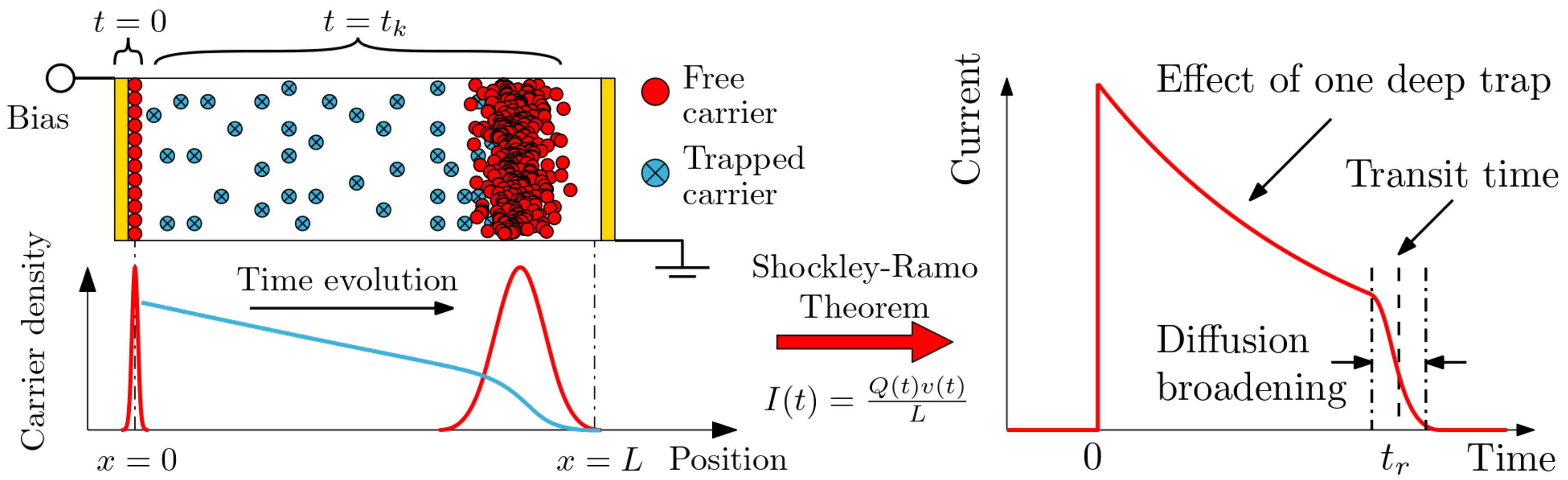

Effects influencing current waveform

Diffusion

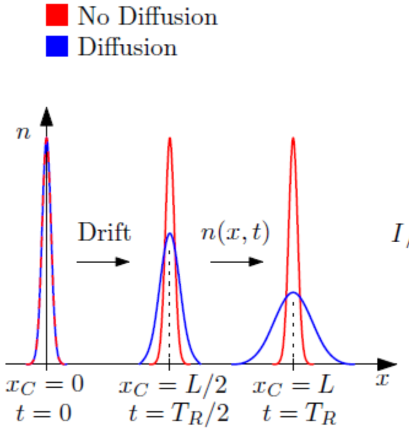

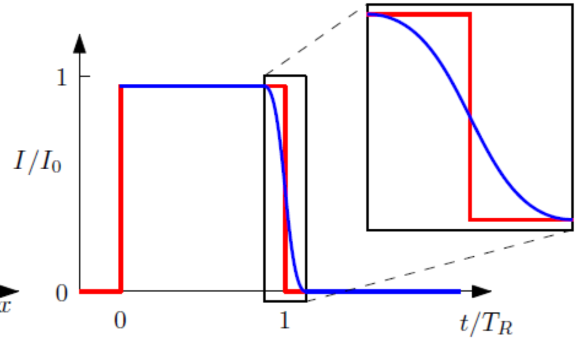

Trapping and de-trapping

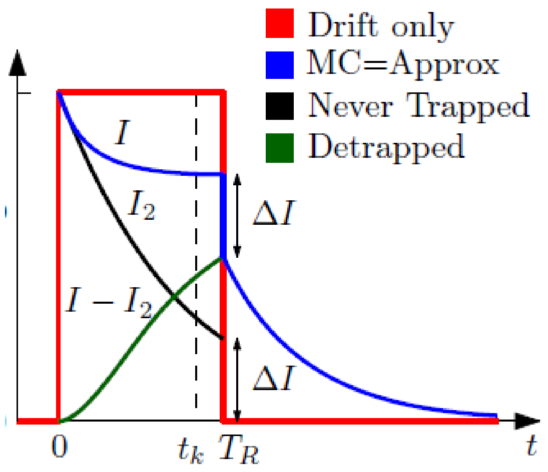

$$\tau_T = \frac{1}{N_T \sigma_c v_{th}},$$

$$\tau_D = \frac{1}{N_C \sigma_c v_{th}} \exp\left(\frac{E_T}{k_B T}\right).$$

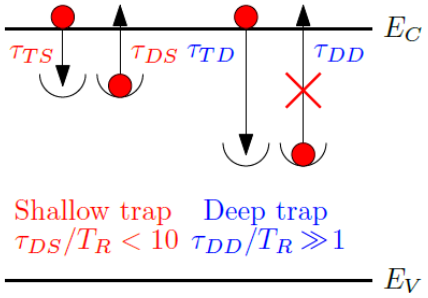

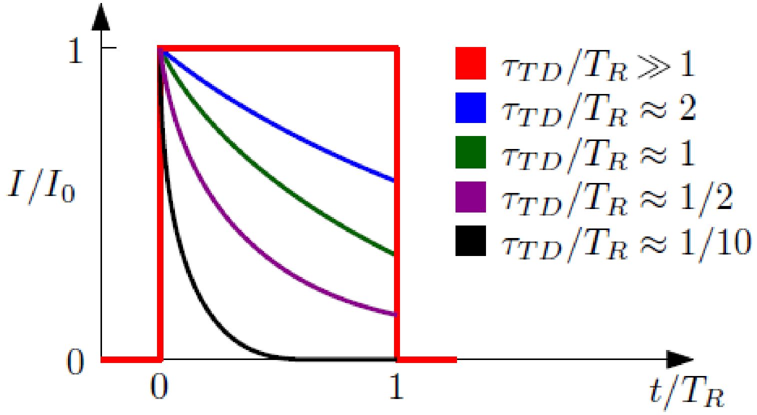

Space charge

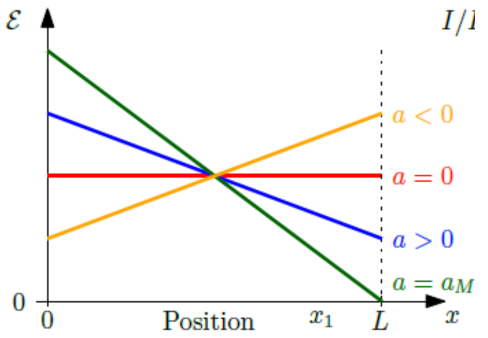

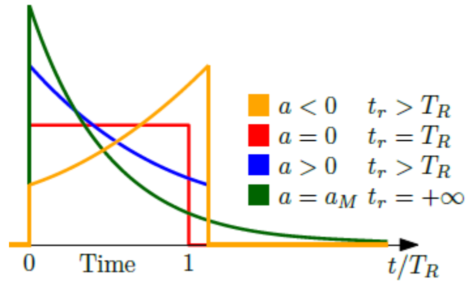

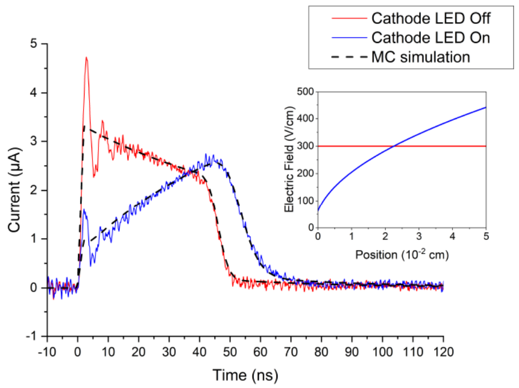

RTSD Workshop, Milano, November 10, 2022

Space charge elimination

- Space charge deteriorates detector performance
- Without bias the detector is neutral
- Space charge formation starts after bias application
- Space charge can be eliminated using **pulsed bias** and effects of space charge can be distinguished from effects of traps
- Changing the laser pulse delay allows study of space charge evolution

Synchronization of laser pulse and bias pulse

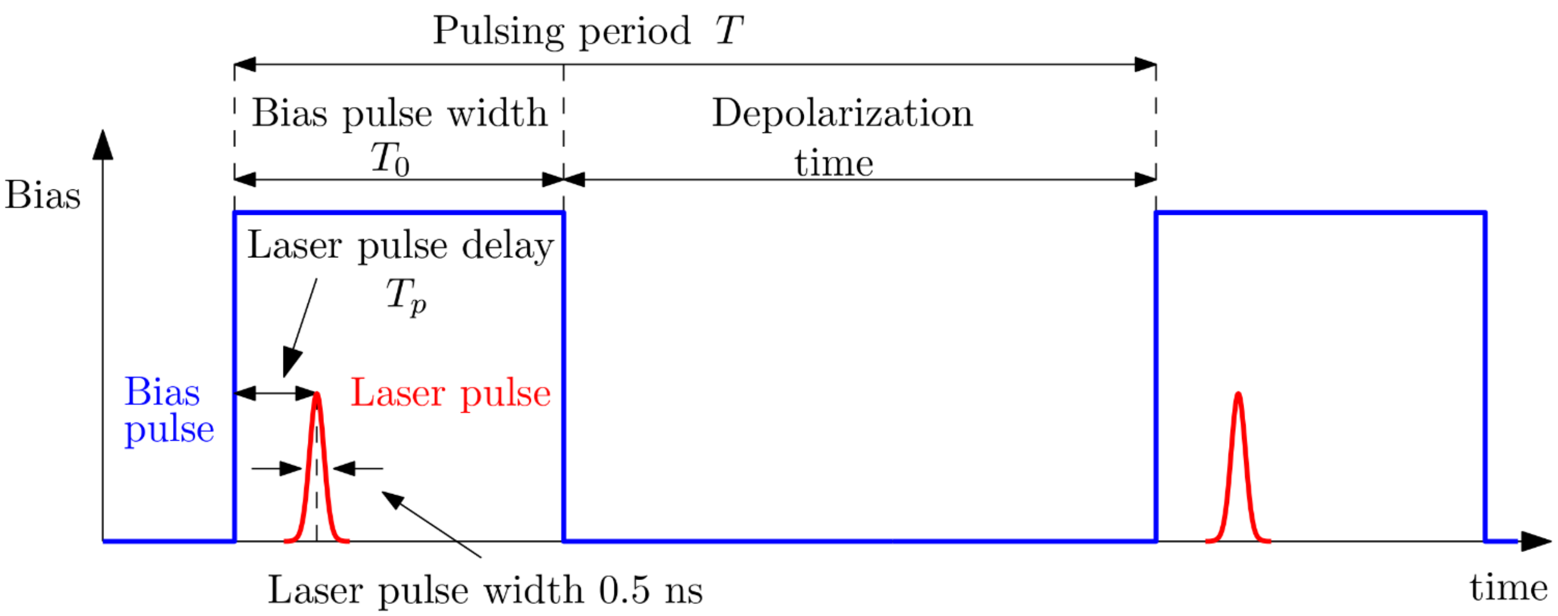

CdZnTeSe - L-TCT measurement results

- Semi-insulating p-type $\mathbf{Cd_{0.9}Zn_{0.1}Te_{0.96}Se_{0.04}}$ sample is used
- L-TCT is combined with pulsed bias to study space charge dynamics

Sample geometry

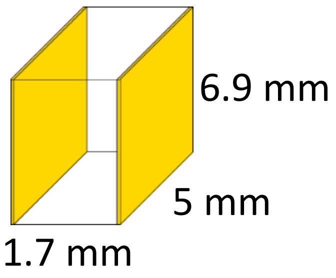

Synchronization of laser pulse and bias pulse

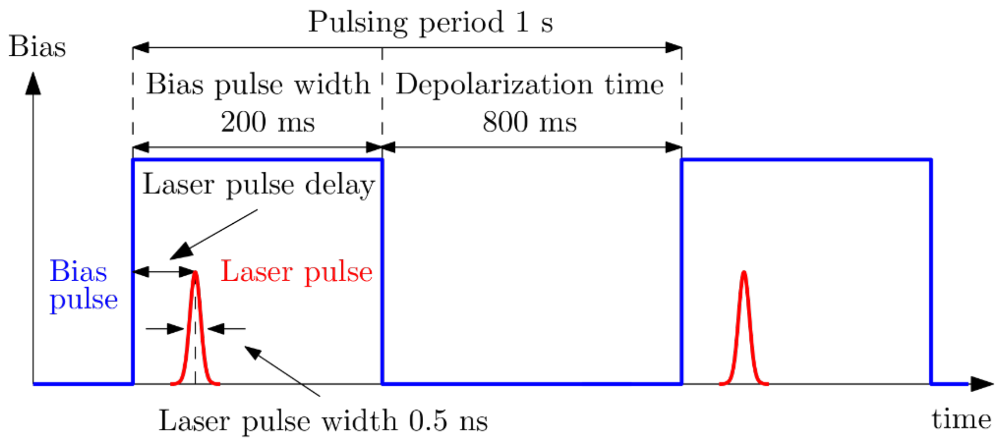

Electron-current waveforms

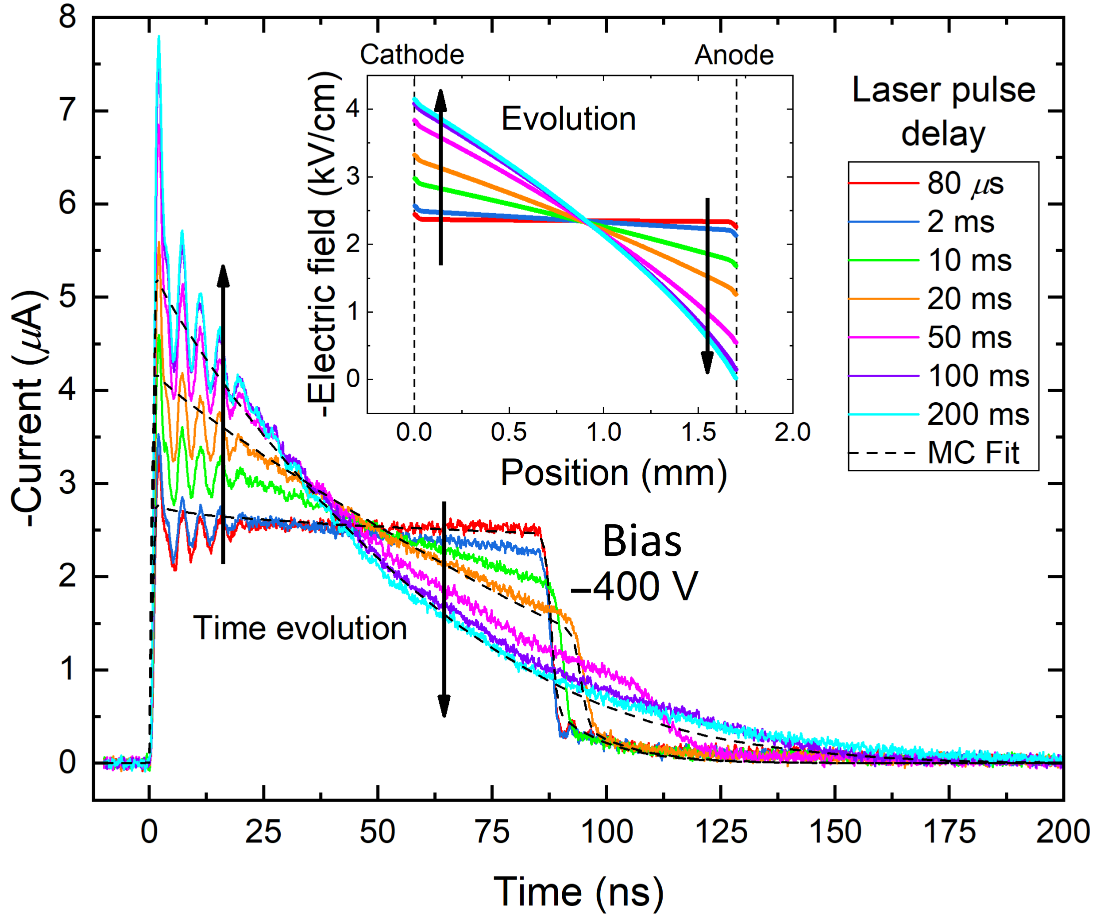

Space charge dynamics

- Three defect levels are sufficient to describe all observed effects
- Positive space charge forms due to hole injection from anode combined with **recombination level** near Fermi level
- Shallow levels do not contribute to space charge

Band diagram

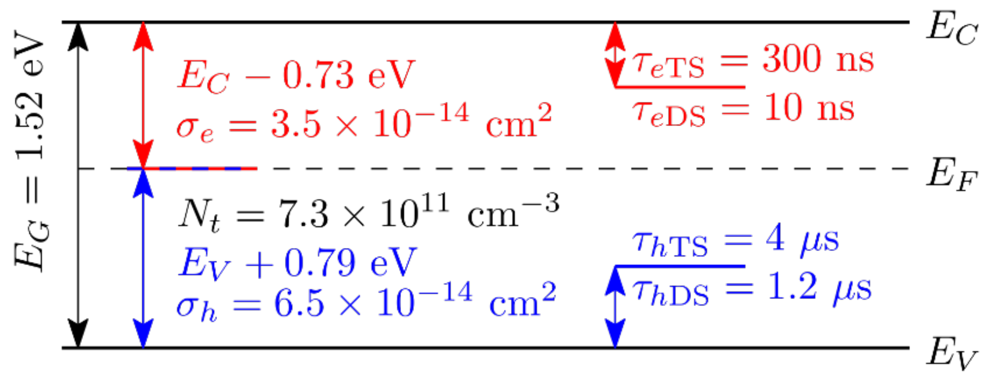

Electric field profile

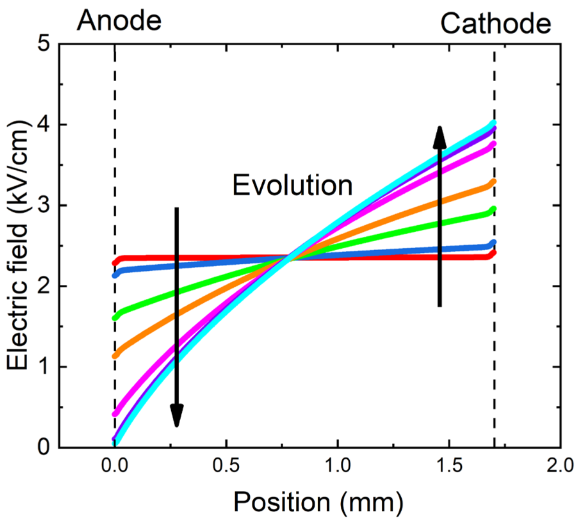

Space charge profile

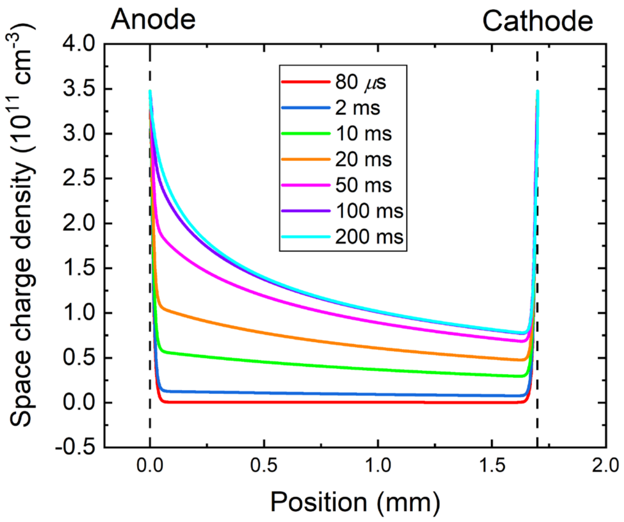

Mean space charge evolution

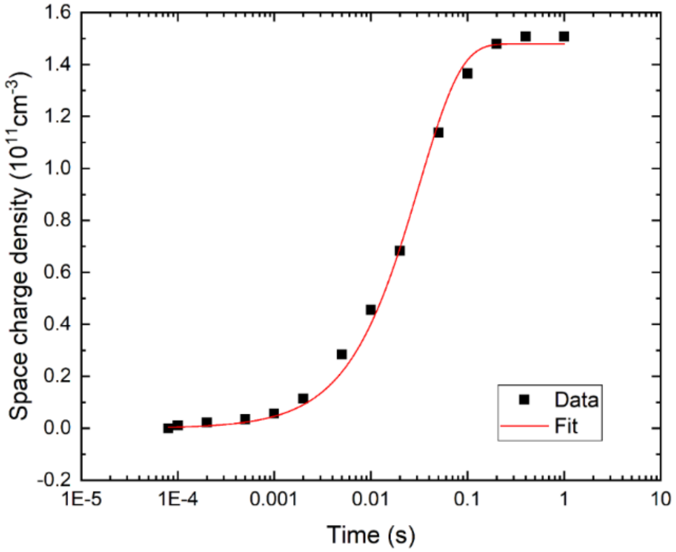

Evaluated parameters

- Same experiment was measured with positive bias for holes
- Identical electric field profile is obtained

- **Evaluated parameters are:**
- Electron mobility μ_e = 830 cm²/Vs
- Hole mobility μ_h = 40 cm²/Vs
- Electron lifetime τ_e = 2.3 µs
- Hole lifetime τ_h = 3.6 µs
- Three defect levels:

Band diagram

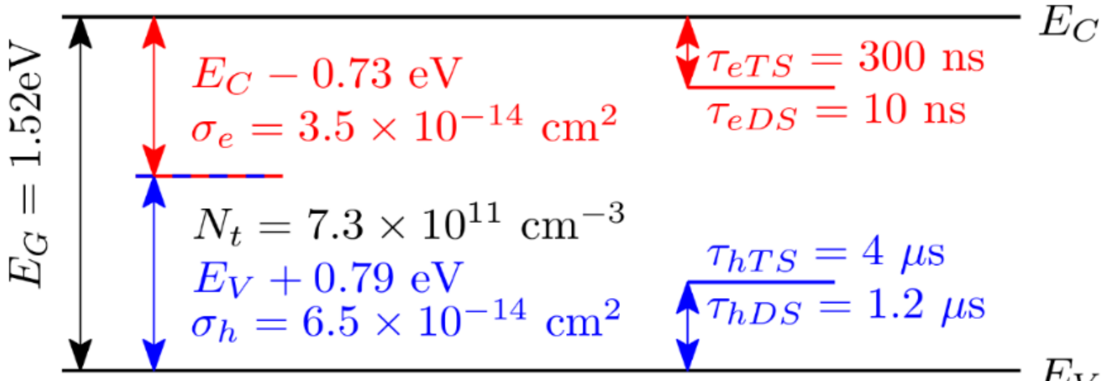

Hole-current waveforms

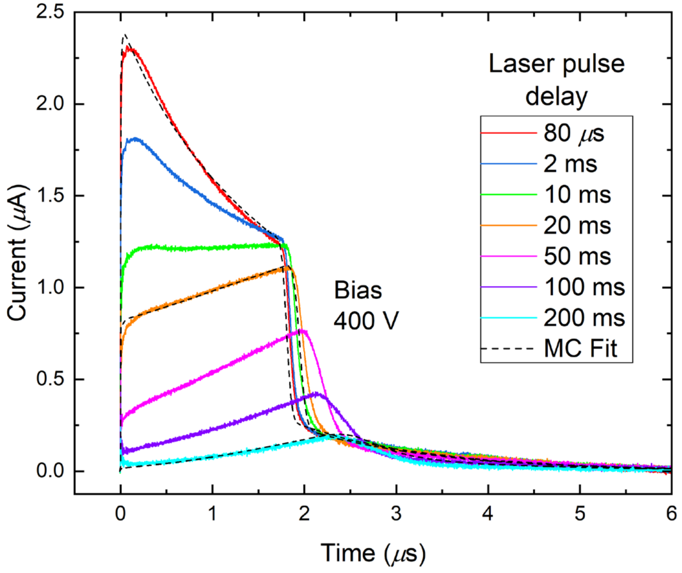

Electric field profile

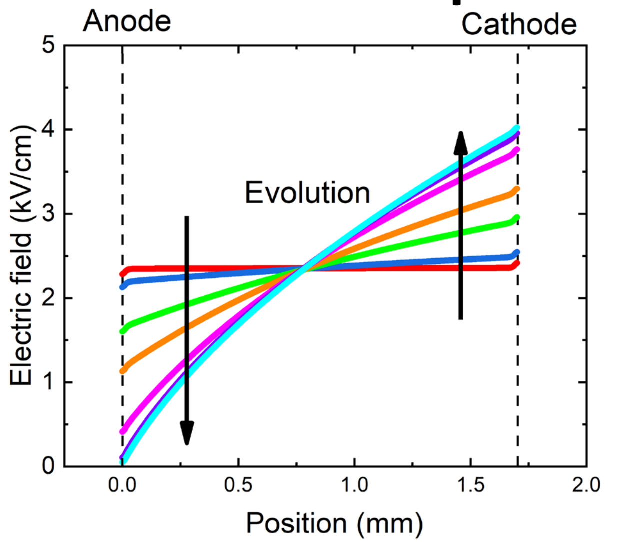

Origin of deep levels

60° Cd core glide dislocation in the (111) plane – first principles calculations

Due to a small concentration of deep levels is an experimental investigation of their origin difficult

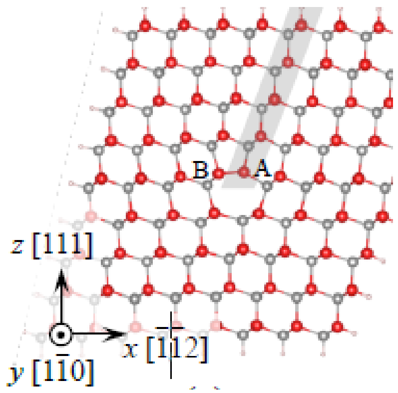

Possible sources:

- Native defects and their complexes ($V_{Cd}, Te_{Cd}, \ldots$)
- Impurities
- dislocations

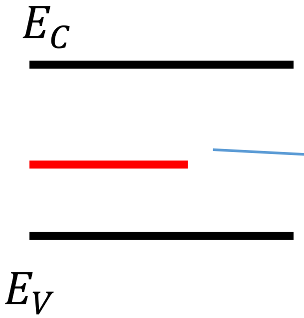

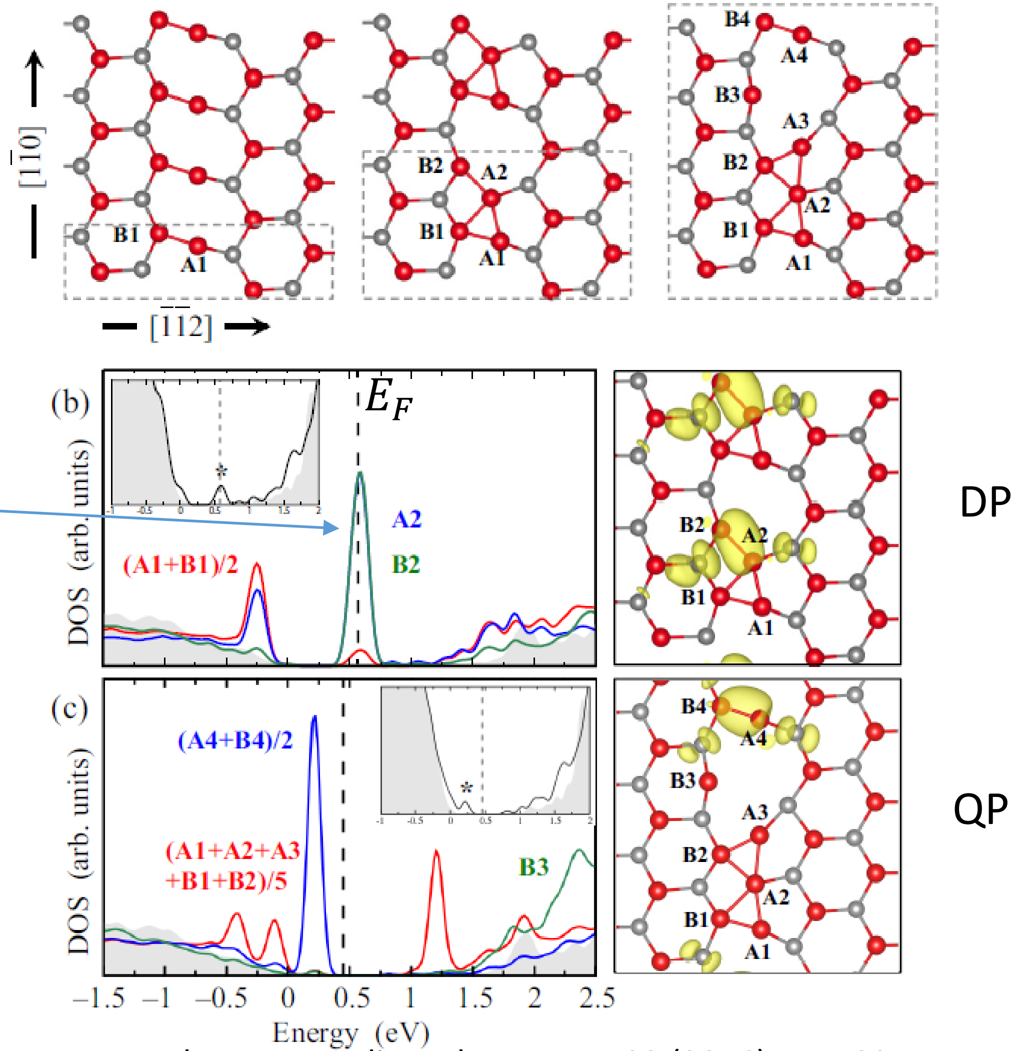

Theoretical calculations of DOS show that dislocation-related deep levels can act as recombination and trapping centers and their position in the gap agree with experiment.

Kweon K.A, Aberg A., Lordi V., Phys. Rev. B 93 (2016) 174109, https://doi.org/10.1103/PhysRevB.93.174109

Vickers microhardness

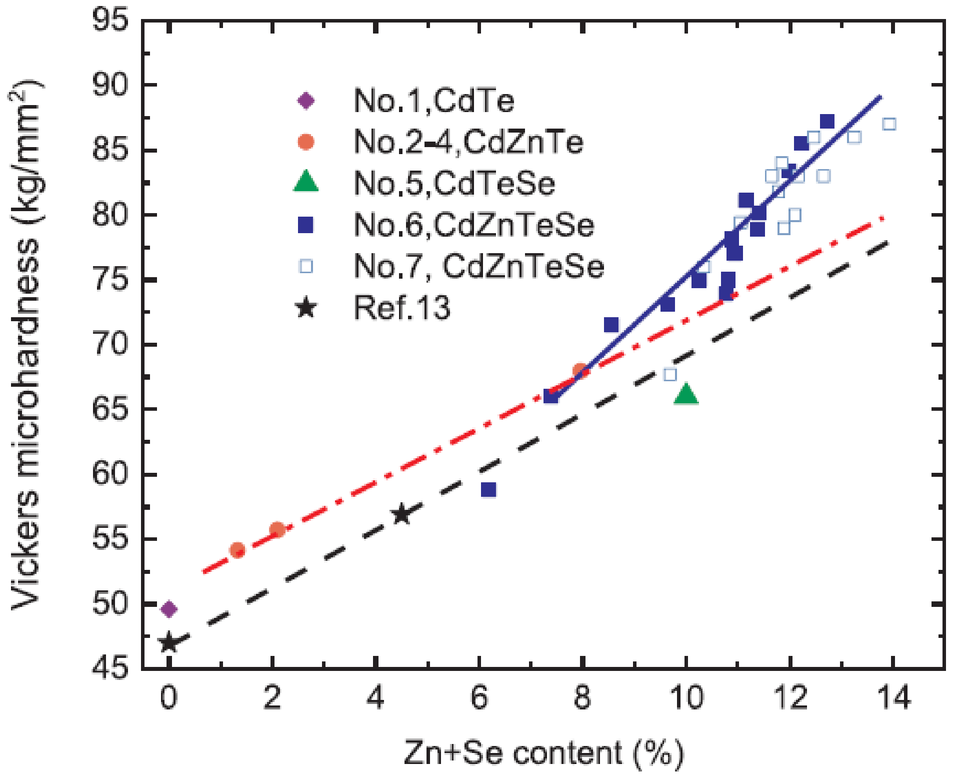

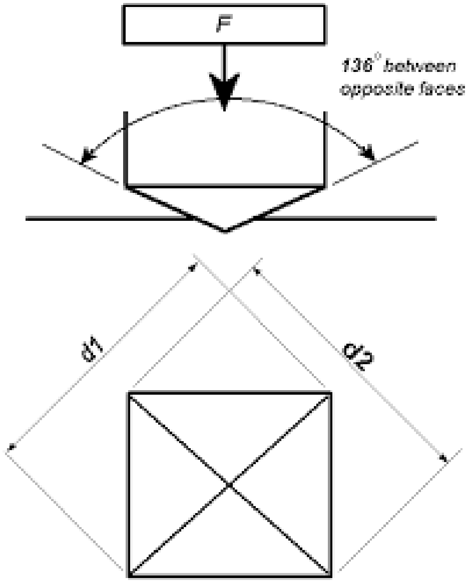

LED or white laser
with bandpass filter

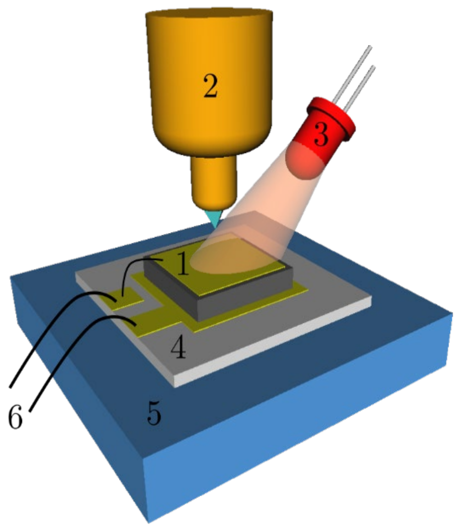

Modified setup – measurement of microhardness with illumination and/or applied bias

This result shows that Se plays a major role in an effective solution hardening of the CZTS matrix and indicates a possible additional strengthening of the effect when Zn and Se are mixed in the CdTe lattice.

Bias dependence of photo plasticity

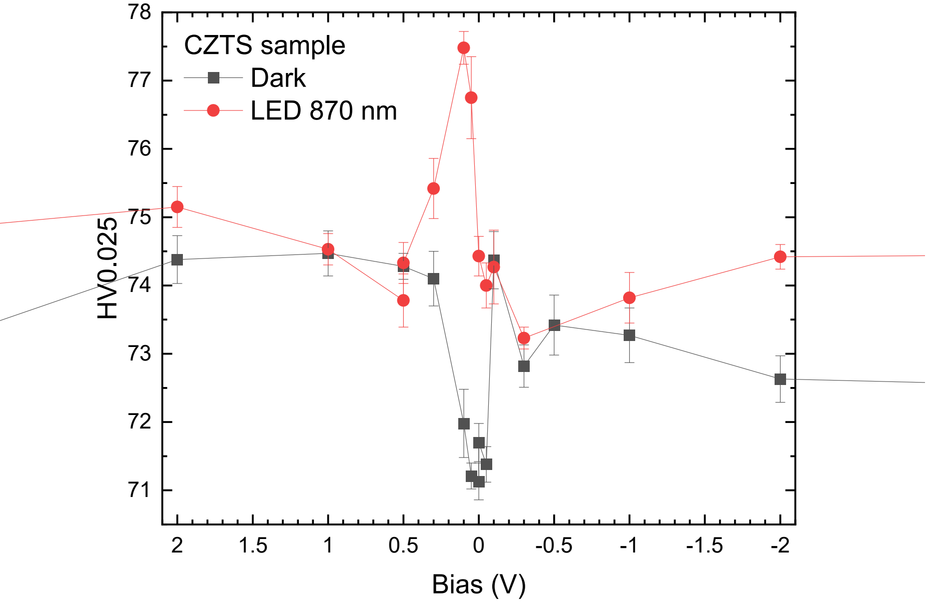

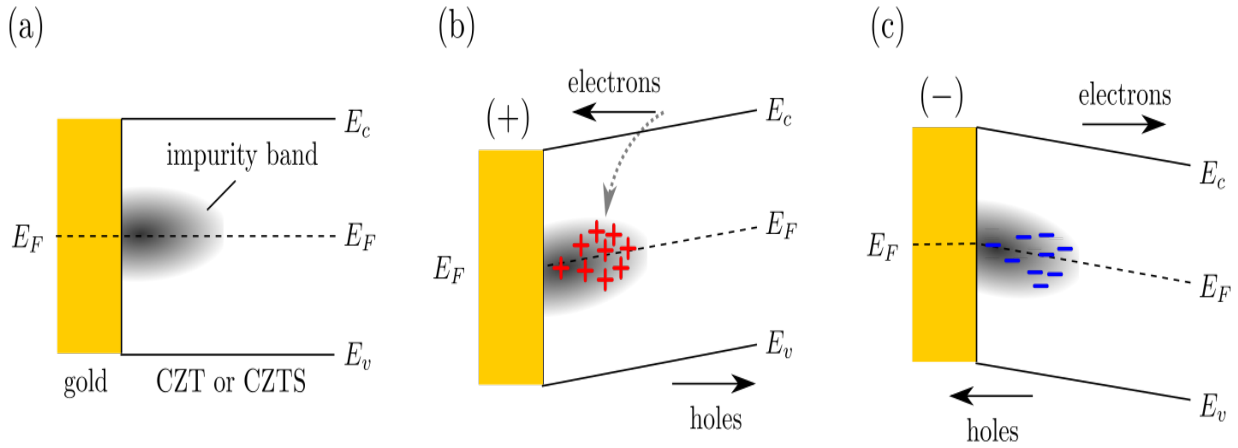

Illuminating the sample leads to the generation of an excessive amount of free carriers that can be captured by dislocation segments according to their electrical character, resulting in dislocation reconstruction and ensuing hardening of the material

In the case of an applied bias, the deformation-induced defect states are filled by the charges from the adjacent contact, while the opposite charge is not supplied by the bulk). One of the charge types (positive/negative) starts to dominate the other one. Subsequently, only appropriate dislocation segments may pass the reconstruction. Due to this reason, the hardness stabilizes near the middle of the hardness at 0 V in the dark and for the illumination

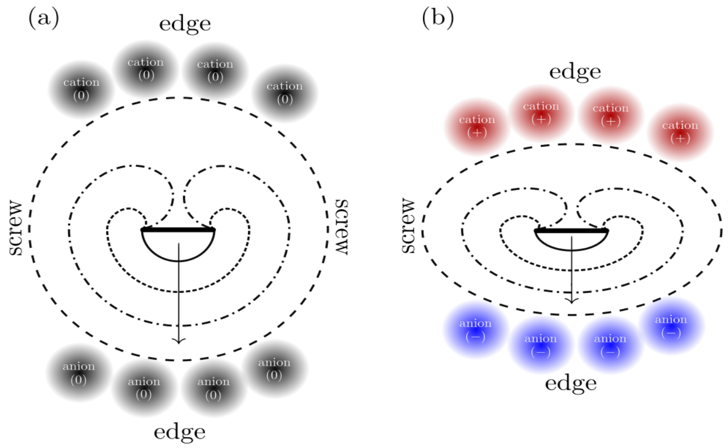

The cation-rich and anion-rich regions accumulate at the opposite sides of the dislocation source. Uncharged dislocations outlined in the left panel (a) glide more easily than charged dislocations shown in the right panel

Spectral dependence of photo plasticity

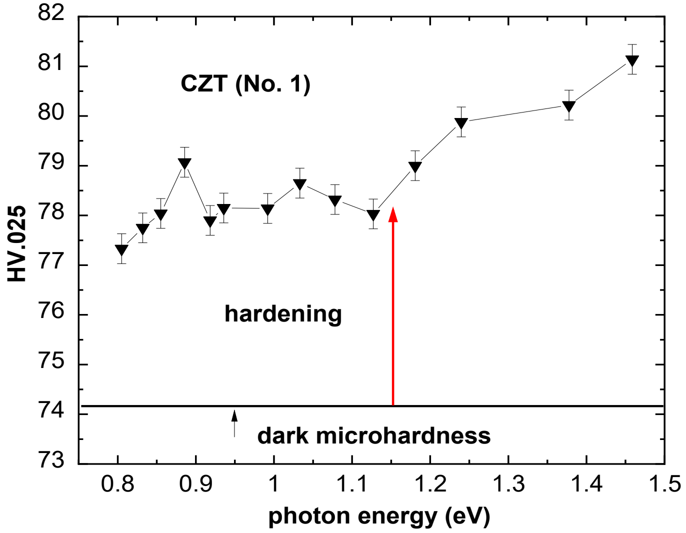

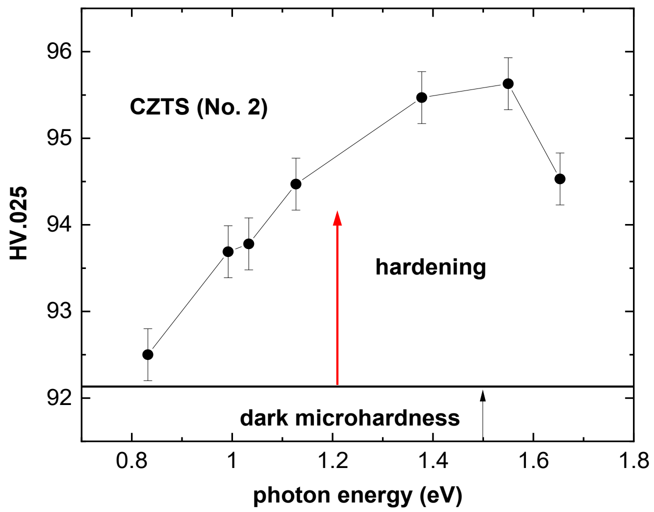

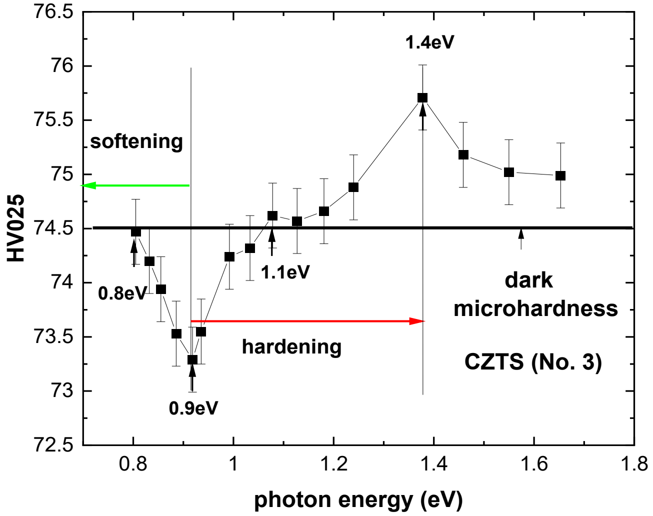

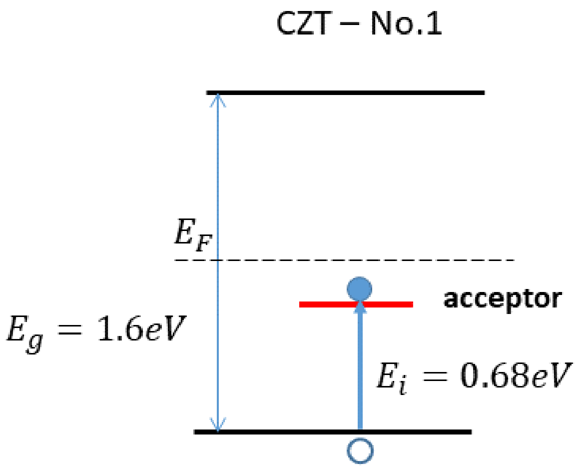

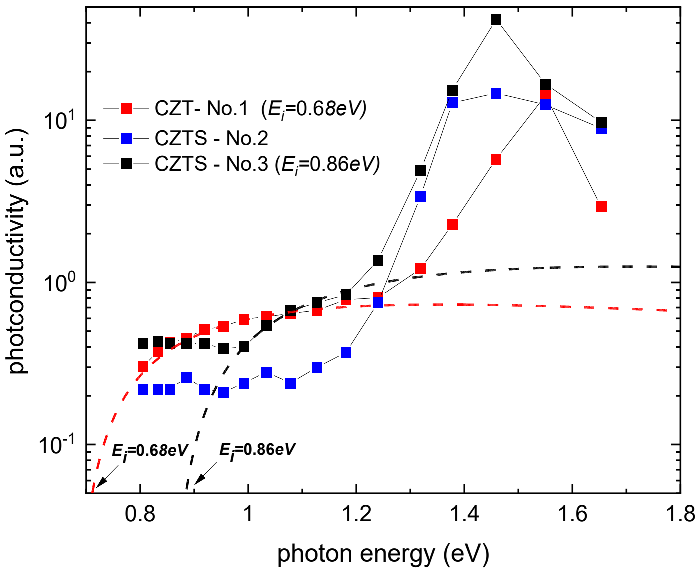

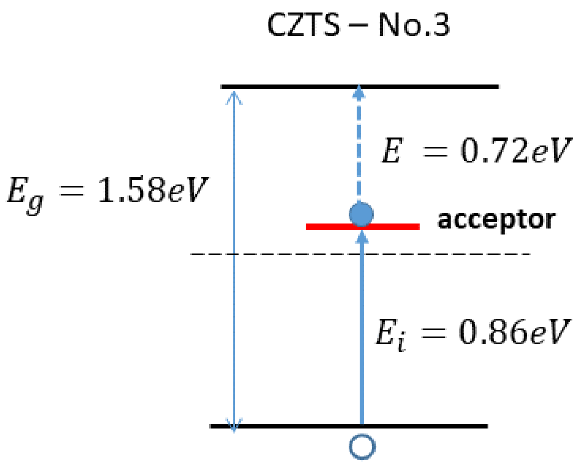

Defects in hybrid perovskites

Methylammonium halide perovskites, $MAPbI_3$, $MABrI_3$

Materials with large application potential – photovoltaics, LED, FET, X-ray and gamma-ray detection

Issues to be solved - stability and defect control

Hole transport $MAPbI_3$ – TCT method

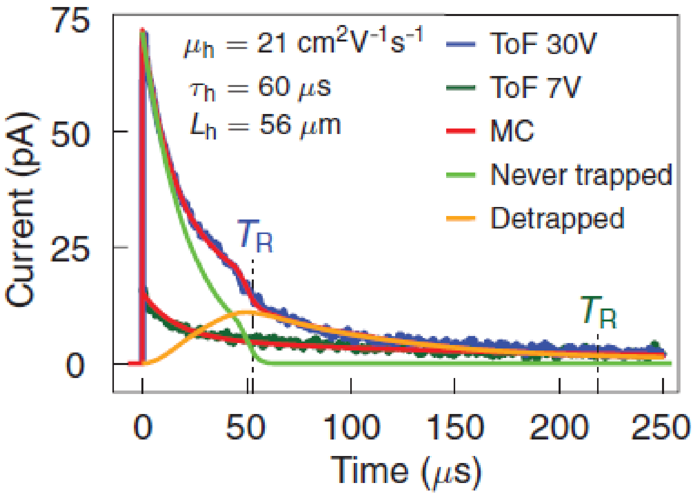

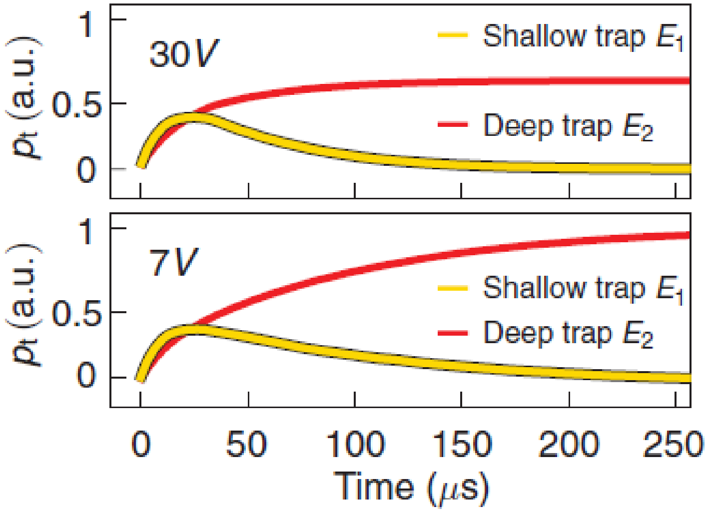

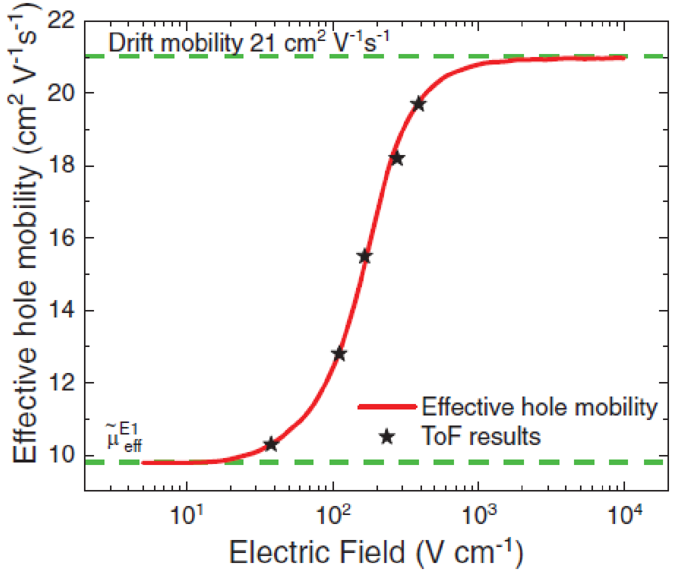

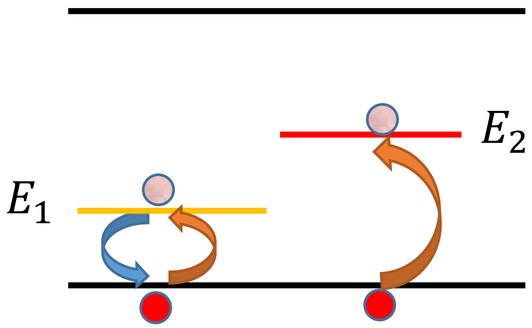

E_1 is responsible for fast trapping ($\tau_t = 3.5\mu s$) and de-trapping ($\tau_t = 4\mu s$) resulting in reduction of effective hole mobility $\mu_{eff} = \dfrac{\mu_e}{1+\frac{\tau_D}{\tau_t}}$

E_2 permanently traps free holes ($\tau_t = 60\mu s, \tau_D$ » $20ms$) resulting in reduction of effective hole mobility

A. Musiienko, D.Cerrati, J. Pipek et al, Adv. Func. Mat. 2021, 31, 2104467

Electron transport $MAPbI_3$ – TCT method

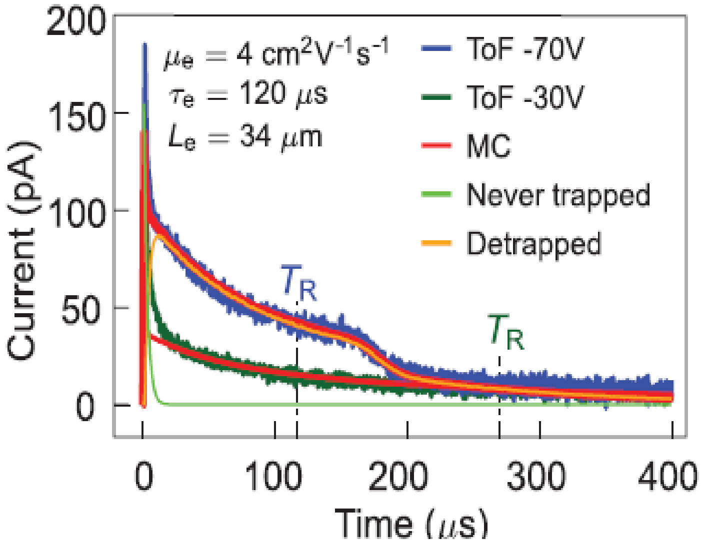

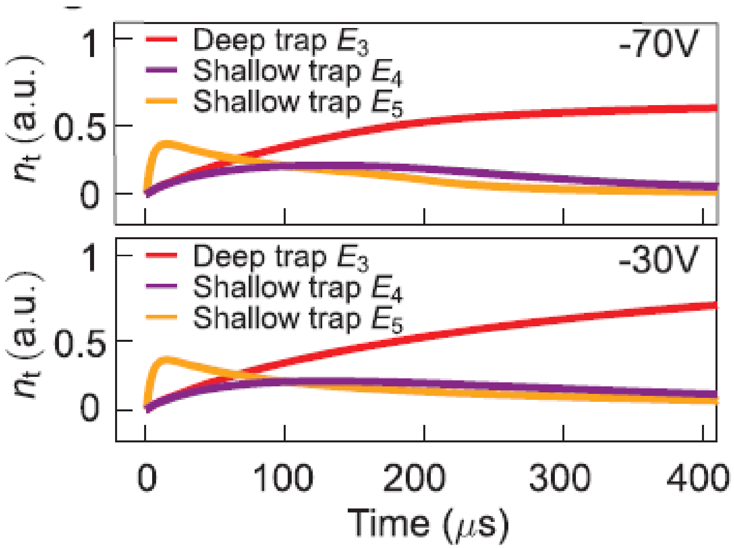

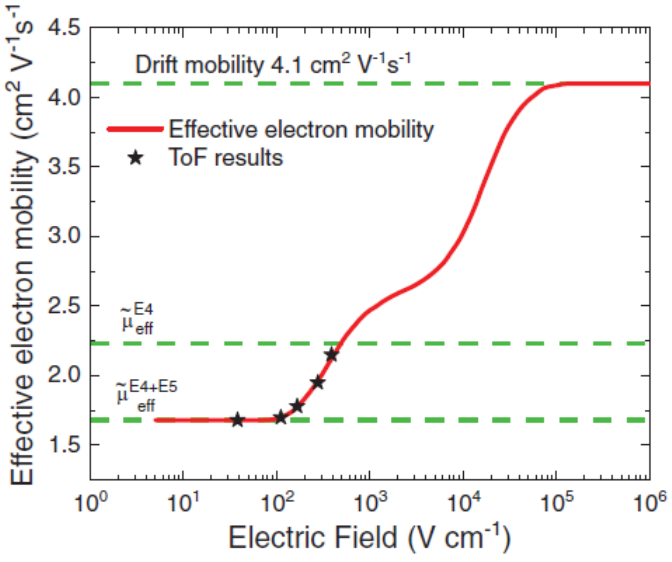

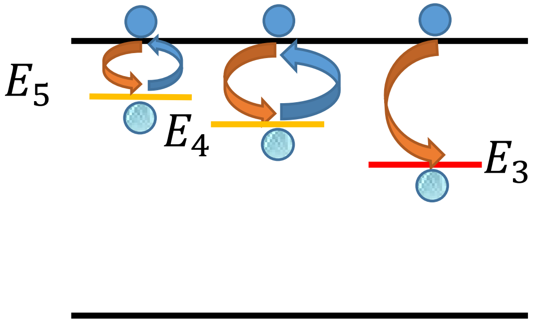

E_4 and E_5 are responsible for fast trapping $\mu_{eff} = \dfrac{\mu_e}{1+\frac{\tau_{D4}}{\tau_{t4}}+\frac{\tau_{D5}}{\tau_{t5}}}$

E_3 permanently traps free electrons ($\tau_t = 120\mu s, \tau_D$ » $20ms$) resulting in reduction of effective hole mobility

A. Musiienko, D.Cerrati, J. Pipek et al, Adv. Func. Mat. 2021, 31, 2104467

Space charge formation nad relaxation in $MAPbBr_3$

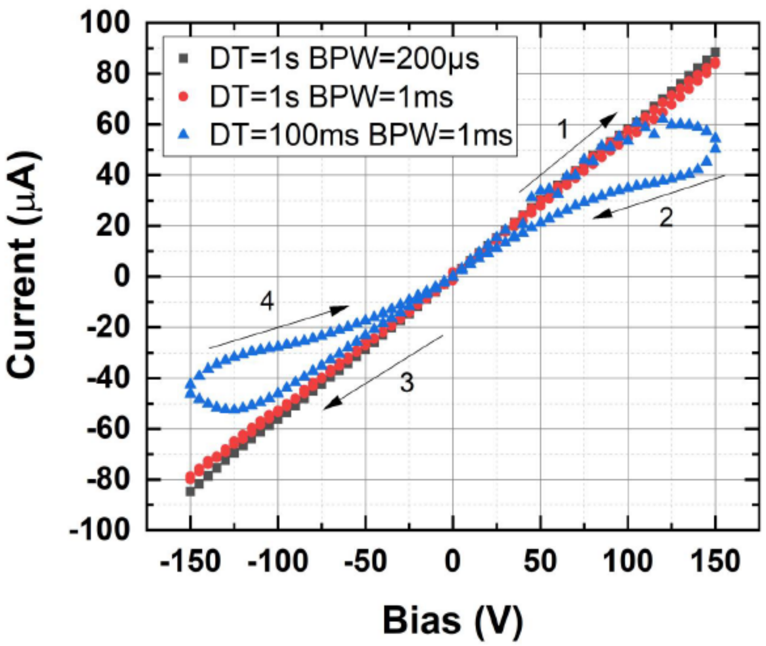

Polarization effects observed

Two models to explain:

1. Ion migration
2. Trapping of carriesr at deep levels

M. Betušiak, poster RTSD-05-326

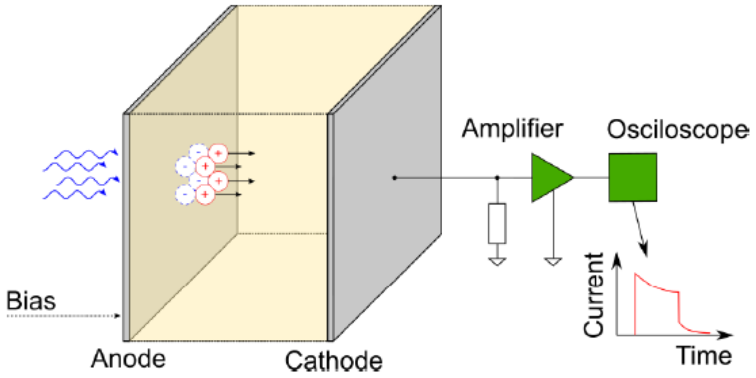

Scheme of our L-TCT setup

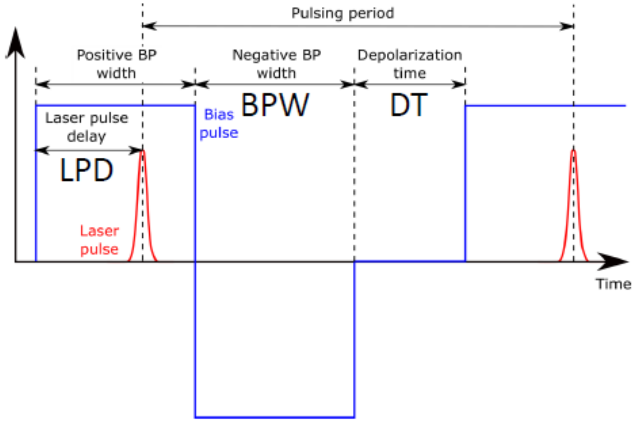

Laser and bias pulse synchronization

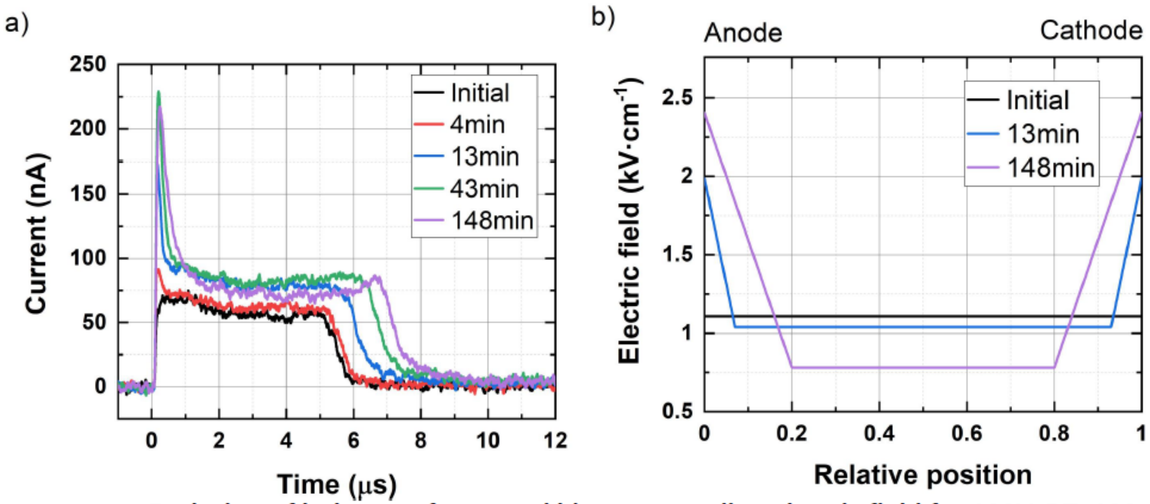

Evolution of hole waveforms and b) corresponding electric field for 100V, DT=100ms BPW=1ms and LPD=100µs.

Level comparison

CdZnTeSe group

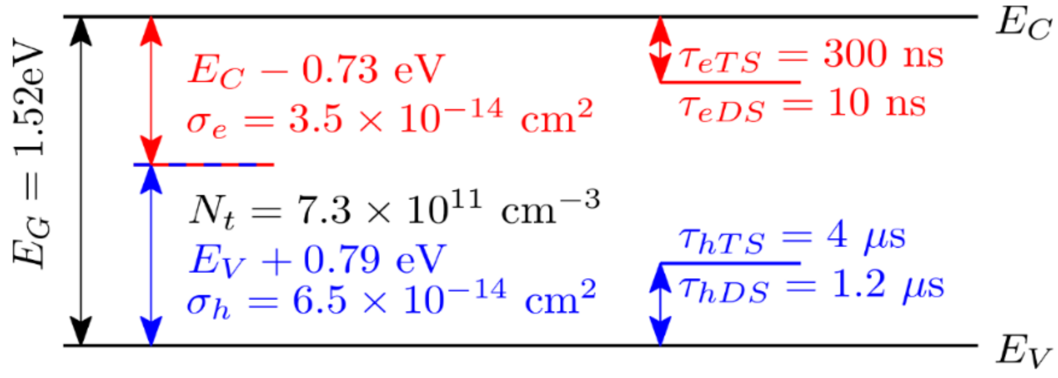

$$\mu_{eff,e} = \frac{\mu_e}{1 + \frac{\tau_D}{\tau_t}} = \frac{\mu_e}{1 + \frac{10}{300}} = 0.967\mu_e$$

$MAPbI_3$

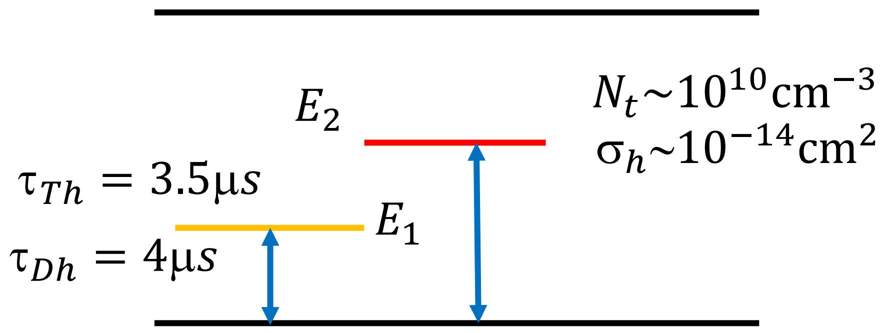

$$\mu_{eff,h} = \frac{\mu_e}{1 + \frac{\tau_D}{\tau_t}} = \frac{\mu_e}{1 + \frac{4}{3.5}} = 0.467\mu_e$$

Midgap level - similar concentration, trapping activity potentially leading to polarization

Shallow traps – in both cases the effective mobility is decreased by trapping at de-trapping at deep levels. The effect is stronger in measured perovskites samples

Future work

Development of L-TCT setup (temperature dependence measurements) and its applications to perovskites, CdTe group compounds, and other materials

Development of Pockels effect method - measurements of graphene/SiC structures, perovskites etc.

Continue to study mechanical properties – Vickers indentation, AFM - CdTe group, perovskites

Thank you very much for your attention